JAERI-M
82-217

POLOIDAL FIELD DISTRIBUTION STUDIES IN TOKAMAK REACTOR

January 1983

Kojyu UEDA*, Satoshi NISHIO, Noboru FUJISAWA
Masayoshi SUGIHARA and Seiji SAITO**

日本原子力研究所
Japan Atomic Energy Research Institute

JAERI-M レポートは，日本原子力研究所が不定期に公刊している研究報告書です。
入手の問合わせは，日本原子力研究所技術情報部情報資料課（〒319—11 茨城県那珂郡東海村）あて，お申しこしください。なお，このほかに財団法人原子力弘済会資料センター（〒319—11 茨城県那珂郡東海村日本原子力研究所内）で複写による実費頒布をおこなっております。

JAERI-M reports are issued irregularly.
Inquiries about availability of the reports should be addressed to Information Section, Division of Technical Information, Japan Atomic Energy Research Institute, Tokai-mura, Naka-gun, Ibaraki-ken 319—11, Japan.

編集兼発行　日本原子力研究所
印　　刷　日立高速印刷株式会社

JAERI-M 82-217

Poloidal Field Distribution Studies in Tokamak Reactor

Kojyu UEDA*, Satoshi NISHIO, Noboru FUJISAWA

Masayoshi SUGIHARA and Seiji SAITO**

Division of Large Tokamak Development,
Tokai Research Establishment, JAERI

(Received December 24, 1982)

On the design studies with the INTOR plasma equilibrium and poloidal field coil configuration (PFCC) from the Phase I to the Phase II A have been obtained the following main results.

Three optimized PFCCs have been obtained: the INTOR-J "Universal" with the optimized PFCC for the divertor configuration, the optimized PFCC for the pump limiter, and the INTOR "Universal" with the PFCC defined as the INTOR reference. These PFCCs satisfy with the requirements for the porthole size for the remote assembly and maintenance of the device, and the maximum flux swing and current densities of the solenoidal coils.

The INTOR-J "Universal" will be almost the same as the INTOR "Universal" in the reactor size. But the optimized PFCC for the pump limiter will be a little larger than the above two configuration because of being in need of slightly larger radii on the two large coils if the plasma with 1.5 in elongation is unconditionally necessary.

The total sum of absolute currents with PFCC, which is used as a parameter for its figure of merit, is found to be given in a range of 80∿90 MAT at high beta for the divertor configuration for both of the

---

* On leave from MITSUBISHI Electric Co., Tokyo

** On leave from HITACHI Co., Hitachi

INTOR-J "Universal" and the INTOR "Universal". The optimized PFCC for pump limiter has 70∿80 MAT in its range. The INTOR-J "Universal" and the INTOR "Universal" for the pump limiter will have its larger sum than one optimized for pump limiter by several MAT.

The "EF only" method, where the flux, Ψ_p, necessary for maintaining the plasma current on high beta is provided only by EF coils, seems to give the total sum a little less than the "EF + OH" method using EF and OH coils for Ψ_p.

The outermost contour (OMC) of scrape-off layer , which is defined so as to have 10 cm at the distance from the plasma surface on its medium plane of the outboard side, is found to require about 30 cm at the distance from its surface on the inboard side. This property is hold on both of the divertor and pump limiter configuration and then the above OMC of scrape-off layer has been used as the INTOR reference.

Keywords : INTOR , Equilibrium Plasma , INTOR-J ,
Poloidal Coil Configuration , Divertor Plasma ,
Pump Limiter

トカマク核融合炉におけるプラズマ平衡およびポロイダルコイル配置

日本原子力研究所東海研究所大型トカマク開発部
上田　孝寿*・西尾　　敏・藤沢　　登
杉原　正芳・斉藤　誠次**

（1982年12月24日受理）

ＩＮＴＯＲ PhaseⅠからPhaseⅡAにわたって研究されたプラズマ平衡およびポロイダルコイル配置について述べる。

ポロイダルコイル配置は，３種類（ＩＮＴＯＲ－Ｊ“Universal”，ＩＮＴＯＲ“Universal”およびポンプリミタ向にのみ研究されたコイル配置…“Universal”はポンプリミタおよびダイバータの両方に適用される意味。）について主に研究された。コイル配置は，分解・組立から要請される開口の大きさ，各コイルに要求される最大電流密度，などの条件を満すよう構成される。

ＩＮＴＯＲ－ＪおよびＩＮＴＯＲ向のコイル配置は，ダイバータへの適用を重視して配置される。これ等をポンプリミタに適用する場合，ポンプリミタに要請されるスクレープオフ層の輪郭（Outermost Contoux of Scrape-of Layer)の位置（後述）の選定に依存するが，楕円度，1.5より幾分小さく選ぶ必要があろう。これを補う意味で，第３のポンプリミタ向のコイル配置が研究された。

ＩＮＴＯＲ－Ｊ“Universal”とＩＮＴＯＲ“Universal”とは，ポロイダルコイル配置から想定して同程度の大きさになる。第３のポンプリミタ向のコイル配置の検討によれば，楕円度，1.5で十分にスクレープオフ層に対する要請を満足するには，炉の直径にして数m大きくする必要があろう。高ベータでのダイバータ向の総アンペアターン（Σ｜ＮＩ｜）は，80～90ＭＡＴであり，ポンプリミタの場合は，それより約10ＭＡＴ少ない。

尚，上記のOutermost Contour of Scrape-off Layerの位置は，半径の大きい側でプラズマ表面から約10 cm の位置（第１壁の内面の位置）を通る磁気面と定義される。この磁気面は，半径の小さい側でプラズマ表面から約30 cm の位置を通る。この性質は，ダイバータおよびポンプリミタの両方で保存される。ポンプリミタの場合，この磁気面はプラズマを内に含む閉曲面であることが必要であるという条件を背景に上記の結論を述べた。

---

* 外来研究員：三菱電機

** 外来研究員：日立

Contents

目　　次

1. Introduction

In this report, poloidal field distribution studies[1]~[3] presented for the INTOR Workshops are aggregated and rearranged. They are composed of the plasma equilibrium and poloidal field coil configurations (PFCC) for both of the divertor and pump limiter concepts.

The INTOR conceptual designs are based and performed on a significant constraint that the PFCC of INTOR should not be linked with toroidal field (TF) coils and should be located outside them, in order to facilitate the remote assembly and maintenance.[4] Therefore it is one of main subjects for the INTOR workshops to look for an acceptable fusion reactor in the reactor size and cost.

In the Phase I a single null poloidal divertor is selected for impurity control and ash exhaust, and a double null poloidal divertor as the alternative.[4] At the beginning our effort was devoted to the single null plasma equilibrium which was in an undeveloped level. Basic techniques to obtain desirable solutions from our codes of calculations of the plasma equilibrium were gained in this phase.[2]

On the final stage of Phase I, our studies were directed toward how to make the outermost contour (OMC) of scrape-off layer on the inboard side bring more close to the separatrix, in particular, in the neighbourhood of the divertor. The OMC is 10 cm away from the separatrix on its mid-plane of the outboard side. It is finally found that no remarkable improvement in satisfying the above aim is obtained even if some poloidal coils, which are limited less than several MAT in ampere-turns, are temporarily located on appropriate positions inside the TF coils for such a purpose.

Total sum of absolute currents (or total ampere-turns) of the PFC, which is used as one of parameters for its figure of merit, is considerably

improved on the final stage of Phase I and Phase IIA, and they have become in an acceptable range.

The design studies performed in the Phase IIA are concentrated on the plasma equilibrium and PFCC suitable for the pump limiter configuration, whose plasma equilibrium has no null point in the plasma and scrape-off regions, and is nearly symmetric with the midplane of the plasma. The pump limiter is a comparatively new concept and are expected to have some advantageous points in comparison with the divertor. An extra space produced by replacing the divertor with the pump limiter may lead to some reduction in the reactor size and cost. Additionally, the plasma equilibrium with the pump limiter configuration may be obtained with smaller total sum of absolute currents than for the divertor configuration. Judging from these points, the pump limiter seems to be better than the divertor. The plasma equilibrium and its characteristics are described together with the PFCC in comparison with the divertor.

Requirements for each overall current density of the PFCC are newly added in Phase IIA on taking the feasible current densities in a realistic design into account.[5] The requirements for its current densities are reflected upon both of the divertor and pump limiter configuration.

Methods of equilibrium calculation in this report are described in Section 2.1. Section 2.2. describes some characteristics of the INTOR plasma equilibrium for both of the divertor and pump limiter configurations. Various requirements, which are presented as common bases, for the PFCC design studies are summarized in Section 3.1. Section 3.2 describes an optimization process of coil arrangement and plasma equilibrium. Section 3.3.1 and Section 3.3.2 describe the PFCC for the divertor and pump limiter configurations, respectively.

2. Equilibrium of the INTOR Plasma

2.1 Methods of equilibrium calculation[6]~[8],[2]

The MHD equilibrium of a tokamak plasma satisfies the well-known Grad-Shafranov equation given in the cylindrical coordinates (r,ψ,z) by the following equation.

$$(\partial^2\Psi/\partial r^2) - (1/r)(\partial\Psi/\partial r) + (\partial^2\Psi/\partial z^2) = -\mu_0 r j_\psi \quad , \tag{1}$$

where Ψ, j_ψ and μ_0 are a poloidal flux function, a toroidal current density and a permeability in vacuum, respectively.

The following expression is assumed for j_ψ.

$$j_\psi = f(r,R_p,\beta_p) \cdot g(\Psi,\Psi_s,\Psi_a) \quad , \tag{2}$$

where R_p, β_p, Ψ_s and Ψ_a are a plasma major radius, a poloidal beta, the poloidal flux function on the plasma surface and on the magnetic axis, respectively. f and g are given by the following equations.

$$f(r,R_p,\beta_p) = \lambda r \cdot [1 + (R_p/r)^2 \cdot (\beta_p^{-1} - 1)] \quad , \tag{3}$$

$$g(\Psi,\Psi_s,0) = (\Psi - \Psi_s)^\alpha \quad , \tag{4}$$

where λ is a constant and is determined so that the integral of j_ψ over the plasma cross section gives the plasma current, I_p. α is a constant, too. The plasma current profile is determined by constant α which is called profile factor, hereafter.

Our codes of the plasma equilibrium calculation contain the following expressions for f and g, too.

$$f(r,R_p,\beta_p) = [\lambda' \cdot r + (\mu/r)] \quad , \tag{5}$$

$$g(\Psi,\Psi_s,\Psi_a) = [1 - \{(\Psi_s - \Psi)/(\Psi_s - \Psi_a)\}^2] \quad , \tag{6}$$

where λ' and μ are simple functions of β_p and R_p. In the analysis, Eq.(3) and Eq.(4) are used mainly because of their simple expression.

On assumption that the plasma is represented by a group of ring currents, a solution of Eq.(1) can be obtained, using the integral formula of the Green's function, and expressed by the following form.

$$\Psi = \Psi^p(r,z) + \Psi^e(r,z) \quad , \tag{7}$$

where $\Psi^p(r,z)$ and $\Psi^e(r,z)$ are a poloidal flux function from the plasma current and from the equilibrium field (EF) coil current, respectively.

The representation of $\Psi^p(r,z)$ is given by

$$\Psi^p(r,z) = \int_{\text{plasma}} \phi(r,z,\rho,\eta) \cdot j_\psi(\rho,\eta) d\rho d\eta \quad , \tag{8}$$

where $j_\psi(\rho,\eta)$ is the plasma current density at (ρ,η) on the plasma crossection. $\phi(r,z,\rho,\eta)$ is the Green's function and expressed by the following expression.

$$\phi(r,z,\rho,\eta) = (\mu_0/\pi k)\sqrt{r\rho} \cdot [\{1-(k^2/2)\} \cdot K(k) - E(k)] \quad , \tag{9}$$

where

$$k = 4r\rho/[(r+\rho)^2 + (z-\eta)^2] \quad ,$$

and K(k) and E(k) are the Bessel's function of the first and second kind, respectively.

$\Psi^e(r,z)$ is given by

$$\Psi^e(r,z) = \sum_K \phi\,(r,z,r_k,z_k) \cdot I_k \quad , \tag{10}$$

where $\sum_k$ is the total sum for the EF coils, and (r_k,z_k) and I_k are the

position and current of the k-th EF coil, respectively.

Plasma equilibrium is solved as a free boundary problem. The EF coil currents are modified in such a way that the plasma shape obtained on every iteration fits several scores of points given on a reference contour expressed by

$$r = R_p + a\cos(\theta + \gamma \cdot \sin\theta) \ ,$$
$$z = K \cdot a \cdot \sin\theta \ , \tag{11}$$

where a and K are the plasma minor radius and elongation, respectively. θ is poloidal angle to be changed from 0 to π. Triangularity can be written in a form of $\delta = \sin\gamma$, and is nearly equal to γ on $0 \leq \gamma \leq 0.4$.

The optimization process of the EF coil currents is performed so as to minimize the square, ε, of the difference between a flux function, $\Psi_0(r_0,z_0)$ given at (r_0,z_0), and the flux function, $\Psi_j(r_j,z_j)$ obtained at each point defined on the reference contour which is composed of a few scores of points, (r_j,z_j) $(j = 1,2,---,M)$. Usually, the point, (r_0,z_0) is a limiter point on the reference contour.

The ε is given by the following,

$$\varepsilon = \sum_j^M w_j\left[\Psi_j - \Psi_0 + \sum_k^N (\phi_{jk} - \phi_{ok})\delta I_k\right]^2 \ , \tag{12}$$

where w_j is a weight function and δI_k is the corrected fraction of current in the k-th EF coil. ϕ_{jk} is defined as $\phi(r_j,z_j,r_k,z_k)$ and N is the total number of EF coils.

In our free-boundary MHD equilibrium code, some constraint conditions can be imposed on its minimization, and are shown on the following description.

(1) No constraint

The minimization of ϵ is performed without any constraint. The best fitting solution to a reference shape will be obtained from this option.

(2) Constraint on the flux supplied by the equilibrium magnetic field

The constraint in this case is given by the following expression.

$$\sum_{k=1}^{N} \phi(R_p, z_p, r_k, z_k) - I_k = \text{const.} = \Psi_p/2\pi \quad , \tag{13}$$

where R_p, z_p and Ψ_p are the plasma major radius, the axial coordinate of the plasma center and the magnetic flux of the EF coils within a circle of R_p in radius, respectively. If we want to keep Ψ_p at a value defined in advance, the plasma equilibrium should be analyzed under this constraint. This option provides very useful means specially for a hybrid PFCC.

(3) Constraint on total ampere-turns

In this case each ampere-turn of the EF coils is decided from the equilibrium calculation under the following constraint for total sum of EF coil currents

$$\sum_{i=1}^{N} N_i I_i = \text{const.} = C_1 \tag{14}$$

The physical meaning of this constraint is not clear except the case of $C_1 = -I_p$, where the total sum of the toroidal currents has zero. As it is comparatively easy to obtain equilibrium solutions from this option, this constraint is convenient as an expendient of preliminary survey when no solution can be obtained under the constraint (2).

(4) Constraint on the sum of square[2] ampere-turns

It is this constraint, given by the following that we want to impose on the equilibrium calculations.

$$\sum_{i=1}^{N} |N_i I_i| = \text{const.} = C_2 \quad , \tag{15}$$

But it seems to be difficult to put them successfully in operation. Instead of Eq.(15) the following constraint is imposed,

$$\sum_{i=1}^{N} (N_i I_i)^2 = \text{const.} = C_3 \ . \tag{16}$$

This constraint is one of new options in our codes and may give useful means for the designs of the EF coil configuration on taking some results described later into consideration.

2.2 Some characteristics of its plasma equilirbium

2.2.1 Profile factor, α

The profile factor of plasma current distribution, α defined in Eq.(4), is one of the most influencial parameters on plasma equilibrium because plasma current distribution, plasma internal inductance, safety factor and so forth depend strongly on it. Table 1 indicates dependence of the current density distribution upon α and together upon the poloidal beta, β_p. The plasma internal inductance, ℓ_i, obtained from these distributions, is also shown in the table. It is found that the current density profile becomes more peaked with increasing α or β_p. Additionally, the radial position of its peak increases and increasingly shifts from the peaks of both of plasma pressure and magnetic flux density, with increasing β_p as though its shift seems to disappear on 1.0 in ℓ_i.

Figure 1 shows relation between α and closed flux surface near the main plasma on high beta with the pump limiter. The reference shape of plasma has 1.50 in elongation, 0.15 in upper and 0.1 in lower triangularity. The safety factor on the plasma magnetic axis, $q_{r=0}$ is shown, too. $q_{r=0}$ is selected here to be nearly equal to 1.0 because of the most realizable value. This means to choose about 0.3 in α. Moreover, closed flux surface around the main plasma are found to decrease in its number flux surfaces around the main plasma are found to decrease in its number which is 10 cm away from the plasma surface on its midplane of the outboad side, does not always make a closed flux surface.

In Fig.2 is shown variation of the magnetic surface and separatrix for the divertor configuration with α. The magnetic surface in the scrape-off layer, with increasing α, extends toward the bottom of figure and, on the other hand, the separatrix near the top seems to be considerably improved so as to go better with the reference shape.

2.2.2 Special features

Figure 3(a) shows a simplified PFCC used on the initial phase of its design studies. Some characteristics obtained from this configuration are described in the following.

Figure 4 shows variation of the magnetic surface near the plasma as a function of triangularity of its bottom ($\equiv \gamma_1$), with parameters fixed at 0.20 in triangularlity of its top ($\equiv \gamma_2$), and 1.60 and 1.4 in elongation of its upper ($\equiv K_2$) and lower part ($\equiv K_1$), respectively. It is found that the magnetic outermost flux surface of scrape-off layer does not always surround the main plasma and has some types in relation with γ_1, such as Fig.4(a), (b) and (c).

Figure 5 shows variation of the above magnetic flux surface as a

function of sum of absolute currents ($= \sum_{i=5}^{7} |N_i I_i| \equiv S_\ell$) with the three coils, that is, the Nos.5, 6 and 7 coils in the bottom of Fig.3(a). The effect similar to one obtained by the change of γ_1 is given by the decrease of S_ℓ. This property is one of the features with the INTOR plasma equilibrium.

In Fig.6 is shown variation of the magnetic surface as a function of the total sum of the square ampere-turns of each coil, $\Sigma(NI)^2$. All three cases are found to have almost the same form of magnetic surface. On the other hand, the total sum of the absolute ampere-turn of each coil, $\Sigma|NI|$ increases from about 88 MAT in (a) to about 110 MAT in (c), and, on the other hand, the flux, Ψ_p increases from about -100 Vs to about -50 Vs, on corresponding to the variation from 4×10^2 $(MAT)^2$ to 3×10^3 $(MAT)^2$ in $\Sigma|NI|^2$.

This result suggests that, the larger Ψ_p is selected the smaller $\Sigma|NI|$ is attained. This relation of $\Sigma|NI|$ with Ψ_p is not always found in all of the INTOR PFCC and seems to be dependent upon some EF coil locations.

There are some subjects that should be made reference to. One of them is a problem how much the vertical width of divertor on the inboard side can be reduced in comparison with about 1 m from the above figures. For this purpose, the effect on its width due to two interior coils, which are temporarily located inside the toroidal coils and just near the plasma, is studied. If the interior coils are actually used, they should be made of normal conductor. Therefore, total ampere-turns of the interior coils will be limited less than several MAT.

Figure 7 shows magnetic flux surfaces without and with interior coils. Two cases, A and B, are shown and these total ampere-turns are selected to be equal to 6 MAT. Conclusively, no remarkable improvement on the

vertical width of divertor is attained by the interior coils, while 92.4 MAT in $\Sigma|NI|$ without the interior coils can be reduced to 75.2 MAT with them.

Assuming that the scrape-off layer is 10 cm in the width on the outboard side, the magnetic flux surface is found to pass through a position separated by 30 cm from the separatrix on the midplane of the inboard side. This property is one of the features with the INTOR plasma with the high beta, too.

The above results are described only for the divertor configuration. The pump limiter configuration is also found to have the same properties: the thickness of scrape-off layer on the inboard and outboard side, and dependence of the magnetic flux surface defining scrape-off layer upon triangurality. A property of the pump limiter configuration is shown in Fig.8. It shows dependence of the closed flux surfaces near the plasma upon its elongation. It is found that the area around the plasma occupied by the closed flux surface decreases with increasing K. This feature is similar to dependence of the outermost magnetic flux surface upon triangularity in Fig.4.

3. Design Studies of PFCC

3.1 Requirements

The INTOR conceptual designs are based and performed on an important postulate that its PFCC should not be linked with the toroidal field coils and then should be located outside them, in order to facilitate its remote assembly and maintenance. Therefore, one of the most important factors determining the area occupied by the PFCC and consequently the reactor size, is the TF coil size, in particular, its outer contour. Another requirement for the PF coil location comes from the portwindow size for the remote assembly and maintenance of the torus. That portwindow has several meters in vertical width on both of the upper and lower part of the mechanical midplane outside the TF coils.

Conductor of the PF coils is made of NbTi superconductor and its magnetic field strength should be less than 8T in practical use on taking the existing technical level into account. Therefore, the maximum flux density of the PF coils is designed to be swung within ±8T. The maximum overall current density with each PF coil should be realized within 1 KA/cm^2 for comparatively small PF coils such as the top and bottom coil of the torus, e.g. Nos.2 and 6 in Fig.3(a), and 0.6 KA/cm^2 for large PF coils, e.g., Nos.3 and 7 in Fig.3(a). It is used here as a criterion on the PF coil design.

Further requirements for the equilibrium plasma configuration are given by the following descriptions.

(1) Active null point for the divertor should be located at (4.80^m, -1.70^m) on its configuration such as in Fig.9.

(2) The divertor plasma should have about 1.6 in elongation and about 0.3 in triangularity. The plasma for the pump limiter has been

decided so as to have about 1.5 in elongation and about 0.2 in triangularity on the final stage in the Phase II A.

(3) The OMC of scrape-off layer as the INTOR reference should be at 3.8 m and 6.6 m in the radial coordinate on the midplane, respectively. This has to be hold on both of the divertor and pump limiter.

(4) Location of the point of contact of the plasma with the limiter is preliminary set at $(4.9^{m}, -1.70^{m})$, as shown in Fig.10.

3.2 Optimization of coil arrangement

An optimization process of PFCC can be given by the following description.

Confirmation of the forbidden regions

One of its regions is from the outer contour of TF coils and another is from the porthole of the assembly and maintenance of the torus, as shown in Figs.9 and 10.

Selection and modification of an OH coil configuration

Preliminary OH coil configurations which are appropriately placed outside the TF coil outer contour are modified and improved through a series of repeated procedure to obtain a desired OH configuration satisfying the following needs.

(1) With ampere-turns per unit flux as little as possible.

(2) Without concentrating too much ampere-turns on any special coil.

(3) With stray fields less than 5×10^{-3} T near and within the plasma region.

(4) With the solenoidal coils satisfying the requirement for both of the maximum field strength and overall current density.

Selection and modification of EF coils from the OH coil configuration

The operation of the EF coil configuration may roughly consist of three steps described in the followings.

(1) The first step --- to obtain total ampere-turns or total sum of absolute current as small as possible by adjusting only the locations of top and bottom coils, e.g., the Nos.2 and 6 in Fig.3(a), on keeping the other where they are located at first.

(2) The second step --- to find out some solenoidal coil arrangements consistent with the requirement for its current densities. This procedure for the pump limiter is performed by decreasing the solenoidal current density only by increasing the axial height of current carrying area on keeping the radial width constant. But the PFCC for the divertor needs some special coils on the solenoidal coil area of passive null side, which play an important part on forming the OMC of scrape-off layer, and then it is a little more troublesome than for the pump limiter.

(3) The third step --- Optimization of the plasma and flux surface shape on the basis of the configurations selected on the first and second step. There are various options of the equilibrium calculation codes for it. For the divertor configuration, the shapes of separatrix and OMC are improved by repeated selections of the location and ampere-turns of the special coils, such as the No.5 in Fig.3(a).

(4) The fourth step --- Sensitivity analyses of the total sum of absolute current (or total ampere-turns), the OMC of scrape-off layer and ampere-turns of the solenoidal coils, for only a little modification of large PF coil positions such as the Nos.3 and 7 coil in Fig.3(a).

3.3 The PF coil configuration

3.3.1 Brief discription of progress

From the Phase I by the Phase II A, the bore of TF coils is reduced by about 2 m. Therefore, the top and bottom coils of the PFCC are reduced by about 1 m in these vertical coordinates. The design studies have been concentrated on the PFCC, for the divertor configuration in the Phase I and for the pump limiter in the Phase II A. On the final stage of Phase II A, merits and demerits of both the divertor and pump limiter configurations were studied in order to compare them.

The PFCCs described in the following section consist of three kinds of PFCCs which are referred to the INTOR-J "Universal" in Fig.9, the optimized PFCC for pump limiter in Fig.10, and the INTOR "Universal" in Fig.14, where the term "Universal" indicates PFCC which can be used for both of a pump limiter and a divertor.

3.3.2 Divertor configuration

The PFCC proposed on the beginning of the Phase I is shown in Fig.3(b) and results of its main parameters are shown in Table 2. Fig.4(b) is determined by the equilibrium calculations with the simplified configuration in Fig.3(a). The separatrix and the OMC of scrape-off layer in Fig. 3(a) are given in Fig.11 are almost the same as in Fig.6(a) at high beta. At that time the requirements for the active null point had not been given, and it were presented on its table for reference.

Figure 11 shows dependence of the total sum of absolute currents, $\Sigma|NI|$ and the active null position, (R_N, Z_N) upon the radial position of No.2 in Fig.3(a), R_2. Judging from Fig.11, $\Sigma|NI|$ is found to have the minimum and Z_N has the maximum, at R_Z nearly equal to 5 m. On the other hand, R_N

decrease monotonically with increasing R_2. The maximum in Z_N and the decrease in R_N correspond to the maximum in elongation and the increase in triangularity, respectively. $\Sigma|NI|$ may not be always selected to be equal to its minimum because it should be selected to be consistent with the requirements for elongation and triangularity.

(1) INTOR-J "Universal"

Figure 9 shows the PFCC, presented on the final stage of the Phase I and defined as the INTOR-J "Universal". The 15 coils except the Nos.4∿6, 8∿10, 12, 20∿22 and 25 coils are used as the hybrid coils. The solenoidal coils consist of the Nos.1∿8 and 14∿21 coils.

Main difference between Fig.9 and Fig.3(b) is on the number of solenoidal coils and the vertical position of the top and bottom coils. The solenoidal coils are divided into 16 blocks of coils and satisfying the maximum flux density swing with ±8T, when Ψ_p supplied by the PFCC is about 40.0 Vs and about -60.0 Vs at both of 0 s and 211 s, respectively.

The top and botom coils, that is, the Nos.10 and 11 coils at the top and the Nos.23 and 24 coils at the bottom in Fig.9, are located symmetrically with the mechanical midplane alternatively, and are 6.5 m at the vertical distance from its midplane. This distance is smaller than in the case of Fig.3(b) by 0.8 m.

The radius R_{13} or R_{26} ($R_{13} = R_{26}$) of large coils, that is, the Nos.13 and 26 coils in Fig.9 is reduced by 1 m compared with the Nos.5 and 10 coils in Fig.3(b). This is due to a reason given by the following descriptions. Figure 12 shows dependence of the separatrix and the OMC of scrape-off layer on high beta upon R_{13} (or R_{26}). The separatrix is found to expand toward both sides of the top and bottom in the figure with increasing R_{13} (or R_{26}). Simultaneously, the OMC is expanded toward them, too, and consequently, the scrape-off layer decreases in its thickness.

From these results the case of 11 m in R_{13} (or R_{26}) is selected as a reference for the INTOR-J "Universal".

Plasma equilibria with the low and high beta, obtained from the PFCC in Fig.9, are shown in Fig.13. The plasma size and position are given numerically as follows.

$$R_{min} = 4.13 \text{ m}$$
$$R_{max} = 6.52 \text{ m}$$
$$Z_{max} = 2.50 \text{ m}$$
$$Z_{null} = -1.70 \text{ m}$$
$$R_{null} = 4.72 \pm 0.065 \text{ m}$$

The reference of plasma shape has 1.6 in elongation and 0.40 in triangularity on the null side, and 1.6 in elongation and 0.20 in triangularity on the null-less side.

Table 3 indicates major parameters for the divertor configuration. Its total flux swing is about 100 Vs from 0 s to 211 s. Also the total sum of absolute current at 0.0 s, 5.0 s, 11.0 s and 211.0 s are nearly equal to 68.40 MAT, 95.15 MAT, 81.93 MAT and 94.68 MAT, respectively. Its value on low beta gives almost the same as on high beta at 211.0 s. The ampare-turns with each poloidal coil are shown in Table 4. The above surprising results on low beta can be found to come from increasing ampere-turns of a pair of coils at its bottom with low β_p (or I_p).

Figure 14 shows variation of the typical parameters, i.e., N_1I_1, $N_{23} \cdot I_{23}$, $N_{23} \cdot I_{26}$, $\Sigma|NI|$ and (R_N, Z_N) on high beta as a function of Ψ_p for the divertor of the INTOR-J "Universal". Both of $|N_1I_1|$ and $\Sigma|N \cdot I|$ are found to increase monotonically with increasing Ψ_p. This property is different from the results with $\Sigma|NI|^2$ = constant.

The ampere-turn of one of the solenoidal coils, $|N_1I_1|$ is about

4 MA at 60 Vs in Ψ_p, and it exceeds by ten % more than 1 kA/mm^2 on the requirement for its current densities. The magnetic field strength for 4 MA in its current is a little less than 8T.

A new method described in the followings is used (obtaining the results shown) in Fig.14. Ψ_p in the operational phase other than 0.0 s can be supplied by the following two methods.

(1) "EF + OH" --- Ψ_p is supplied by both of FF and OH coils.

(2) "EF only" --- Ψ_p is supplied only by EF coils.

We have used the "EF only" method for the high beta at 11.0 s, and the "EF + OH" method for both of the low beta at 5 s and high beta at 211 s. In Fig.14, only the "EF only" method is used and the figure contains both high beta cases of 11 s and 211 s.

$\Sigma|NI|$ at the high beta at 211 s obtained from the "EF + OH" method is given in Table 4, and is about 5 MAT more than about 90 MAT in $\Sigma|NI|$ at -60 Vs (corresponding to high beta at 211 s) in Fig.14. From this result, the "EF only" method seems to give smaller $\Sigma|NI|$ on high beta than the "EF + OH" method.

(2) INTOR "Universal"

In Fig.15 is shown the PFCC which is presented on the final stage of the Phase II A as the INTOR "Universal". It consists of 22 PF coils and is 4 blocks of coils less than in Fig.9. In this figure, the vertical positions of a pair of coils at the top and bottom are also reduced by 0.45 m and 0.30 m in comparison with Fig.9, respectively. Moreover, the vertical distance between a pair of large coils is expanded from 9.15 m to 10.00 m in order to satisfying requirements for the large porthole for the remote assembly and maintenance of the device.

In table 5 are shown NI of each coil, $\Sigma|NI|$ and Ψ_p for the INTOR "Universal". The results are shown for both of the "EF + OH" and "EF only"

methods. It is found that only a little discrepancy among the results from them is observed as far as $\Sigma|NI|$ is concernded, except at the high beta at 211.0 s. In the case at 211.0 s, $\Sigma|NI|$ from the "EF only" method is about 8 MAT less than from the "EF + OH" method.

Judging from these results it seems to result in more reduced $\Sigma|NI|$ to select Ψ_p at its high beta as large as possible. This conclusion is also consistent with the trend already described in Fig.6 but is found to be different from the porperty in Fig.14 for the INTOR-J "Universal".

Table 6 indicates major parameters of the PFCC, based on a set of selection: "EF + OH" for low beta at 5.0 s, "EF + OH" for high beta at 11.0 s and "EF only" at 211.0 s. Each plasma shape corresponding to Table 6 is shown in Fig.16.

3.3.3 Pump Limiter configuration

The PFCC for the pump limiter configuration is shown in Fig.10, which is referred to as the optimized PFCC for pump limiter. Each coil of the PFCC is located almost symmetrically with the mechanical midplane. The main difference between this configuration and the divertor configuration, e.g., on the INTOR-J "Universal" lies in its top and bottom coils and the radial positions of two large coils, R_{12} or R_{24} ($R_{12} = R_{24}$).

One of a pair of coils at the top and bottom is reduced in comparison with the divertor configuration on taking smaller EF currents which they will carry on into account.

The relatively large radius, R_{12} (or R_{24}) is selected on the follow- data base. Figure 17 shows dependence of the closed flux surface near plasma upon R_{12} (or R_{24}), with fixed axial coordinates. The reference of plasma shape has 1.5 in both of upper and lower elongation, and 0.15 and 0.10 in upper and lower triangularity, respectively. Number of closed

flux surface between the plasma surface and the OMC of scrape-off layer increase with increasing R_{12} (or R_{24}). The OMC is flux surface which passes through the position, defined on the midplane and being 10 cm away from the main plasma surface on the outboard wall side. It is found that Fig.17(a) for $R_{12} = 11$ m may not have this surface, but Fig.17(b) and (c) for 12 m and 13 m in R_{12}, respectively can have it. Therefore, the pump limiter configuration has the large radius in two large coils. This result is different from the property of the divertor configuration already described in Fig.12.

Table 7 and 8 indicate major parameters and ampere-turns with the PFCC, respectively. The "EF + OH" method is used at low beta and at high beta at 211.0 s. The "EF only" method is used only on high beta at 11.0 s.

The maximum magnetic strength of its solenoidal coils is within ±8T when Ψ_p at 0.0 s and 211.0 s are nearly equal to 40 Vs and -70 Vs, respectively. NI and $\Sigma|NI|$ on each phase from low to high beta are found to be generally less than for the divertor configuration. For example, $\Sigma|NI|$ at 11.0 s is less than in Table 4 (or Fig.9) by about 10 MAT. Figure 18 shows the plasma equilibrium for the pump limiter configuration for low and high beta, with its reference of 1.5 in elongation and 13 m in R_{12} or R_{24}. This is the case which is found to meet the closed OMC of scrape-off layer corresponding to the INTOR reference.

(1) INTOR "Universal"

The PFCC, which is the same as for the divertor configuration and defined as INTOR "Universal" in Fig.14, is attempted to be used for the pump limiter configuration.

Table 9 and 10 indicate major parameters and ampere-turns of each coil of the PFCC, respectively. $\Sigma|NI|$ on each phase from low to high beta is found to be a little more than in Table 7, except at low beta

at 5.0 s. In Fig.19 is shown the plasma equilibrium for this PFCC at the low beta at 5.0 s and the high beta at 11.0 s (or 211.0 s). The plasma at 11.0 s may not have the OMC of scrape-off layer defined as the INTOR reference as though it is not clear in the figure. But it will be obtained at a little sacrifice in the elongation of plasma as known by the trend shown in Fig.8.

(2) INTOR-J "Universal"

The PFCC which has been furnished the divertor configuration as the INTOR-J "Universal" must be used for the pump limiter, too.

Its major parameter and ampere-turns of each coil are given in Table 11 and 12, respectively. In Fig.20 is shown the plasma equilibrium from low to high beta. Its OMC of scrape-off layer is found to be almost the same as from the INTOR "Universal" and the plasma may be required so as to select its elongation a little less than 1.5.

Figure 21 shows variation of the typical parameters, that is, N_1I_1, $N_{23} \cdot I_{23}$, $N_{26} \cdot I_{26}$ and $\Sigma|NI|$ as a function of Ψ_p. In the figure, the EF only method is used. Both of $|N_1I_1|$ and $\Sigma|NI|$ just like the divertor shown in Fig.14 increase monotonically with increasing $|\Psi_p|$. But the ampere-turns with one of the solenoidal coils, $|N_1I_1|$ become about 4 MA at 70 Vs, and this result is different from the case of divertor where 4 MA in those ampere-turns is attained at $\Psi_p = 60$ Vs.

4. Conclusion

On the design studies with the INTOR plasma equilibrium and poloidal field coil configuration (PFCC) from the Phase I to the Phase II A have been obtained the following main results.

Three optimized PFCCs have been obtained: the INTOR-J "Universal" with the optimized PFCC for the divertor configuration, the optimized PFCC for the pump limiter, and the INTOR "Universal" with the PFCC defined as the INTOR reference. These PFCCs satisfy with the requirements for the porthole size for the remote assembly and maintenance of the device, and the maximum flux swing and current densities of the solenoidal coils.

The INTOR-J "Universal" will be almost the same as the INTOR "Universal" in the reactor size. But the optimized PFCC for the pump limiter will be a little larger than the above two configuration because of being in need of slightly larger radii on the two large coils if the plasma with 1.5 in elongation is unconditionally necessary.

The total sum of absolute currents with PFCC, which is used as a parameter for its figure of merit, is found to be given in a range of $80 \sim 90$ MAT at high beta for the divertor configuration for both of the INTOR-J "Universal" and the INTOR "Universal". The optimized PFCC for pump limiter has $70 \sim 80$ MAT in its range. The INTOR-J "Universal" and the INTOR "Universal" for the pump limiter will have larger sum than one optimized for pump limiter by several MAT.

The "EF only" method, where the flux, Ψ_p, necessary for maintaining the plasma current on high beta is provided only by EF coils, seems to give the total sum a little less than the "EF + OH" method using EF and OH coils for Ψ_p.

The outermost contour (OMC) of scrape-off layer , which is defined so as to have 10 cm at the distance from the plasma surface on its medium plane of the outboard side, is found to require about 30 cm at the distance from its surface on the inboard side. This property is hold on both of the divertor and pump limiter configuration and then the above OMC of scrape-off layer has been used as the INTOR reference.

Acknowledgements

The authors would like to express their sincere thanks to Drs. K. Tomabechi , M. Yoshikawa , K. Sako , T. Hiraoka , T. Tone , Y. Seki , and K. Tachikawa for their valuable discussion and continuing encouragement. They also wish to thank all other members of the next reactor design group in the JT-60 planning office , and Dr. K. Shinya in Toshiba Electric Co.,Ltd. for useful discussion and suggestion on the usage and application of the equilibrium codes , and the design studies on poloidal coil configuration.

The outermost contour (OMC) of scrape-off layer , which is defined so as to have 10 cm at the distance from the plasma surface on its medium plane of the outboard side, is found to require about 30 cm at the distance from its surface on the inboard side. This property is hold on both of the divertor and pump limiter configuration and then the above OMC of scrape-off layer has been used as the INTOR reference.

Acknowledgements

The authors would like to express their sincere thanks to Drs. K. Tomabechi , M. Yoshikawa , K. Sako , T. Hiraoka , T. Tone , Y. Seki , and K. Tachikawa for their valuable discussion and continuing encouragement. They also wish to thank all other members of the next reactor design group in the JT-60 planning office , and Dr. K. Shinya in Toshiba Electric Co.,Ltd. for useful discussion and suggestion on the usage and application of the equilibrium codes , and the design studies on poloidal coil configuration.

References

(1) N. Fujisawa, M. Sugihara, K. Shinya and K. Ueda: Report of Physics Group Tasks for IAEA INTOR Workshop, Japan, JAERI October 20-31 (1980)

(2) N. Fujisawa, M. Sugihara and K. Ueda: Report of Physics Group Tasks for IAEA INTOR Workshop, Japan, JAERI Mar.30 - Apr.11 (1981)

(3) K. Ueda, S. Nishio, M. Hatayama, S. Saito, M. Sugihara and N. Fujisawa: Task 1.2.4 in Japanese Contribution for Session IV of INTOR Workshop, Phase II.A, March 22 - April 2 (1982)

(4) "International Tokamak Reactor Zero Phase": Report of the international Tokamak Reactor Workshop organized by IAEA and held in Four Sessions in Vienna 5-16 Feb., 11 June - 6 July, 1-23 Octo. and 10-19 Decem. (1979)

(5) INTOR Summary Report of Session 3 Phase II A Group F: Magnetics and Electromagnetics, December (1981)

(6) H. Ninomiya, A. Kameari and K. Shinya: JAERI-M 9127 (September 13, 1980)

(7) K. Shinya and H. Ninomiya; JAERI-M 9278 (December 22, 1980)

(8) H. Ninomiya, K. Shinya and A. Kameari: Proc. 8th Symp. on Engineering Problems of Fusion Research, Vol.1, 75 (1979)

(9) K. Lackner, W. Schneider and U. Seidel: "Poloidal Field Design for INTOR", December (1981)

(10) O. Gruber and K. Lackner: "Poloidal Field Design Calculations for INTOR Divertor and Limiter Versions" in the Report of European Contributions to the 5th Workshop Meeting on INTOR Phase II A

(11) T.G. Brown, B.A. Cramer, G.M. Fuller, R.J. Kalsi, M.H. Kunselman, P.H. Sager, V.C. Srivastava and C.A. Trachsel: INTOR Reactor Design Studies July (1982)

(12) INTOR Summary Report of Session V Phase II A Group F: Magnetics and Electromagnetics, 12-13 July (1982)

Table 1 Dependence of plasma current density distributions upon form factor, α from low to high poloidal beta, β_p

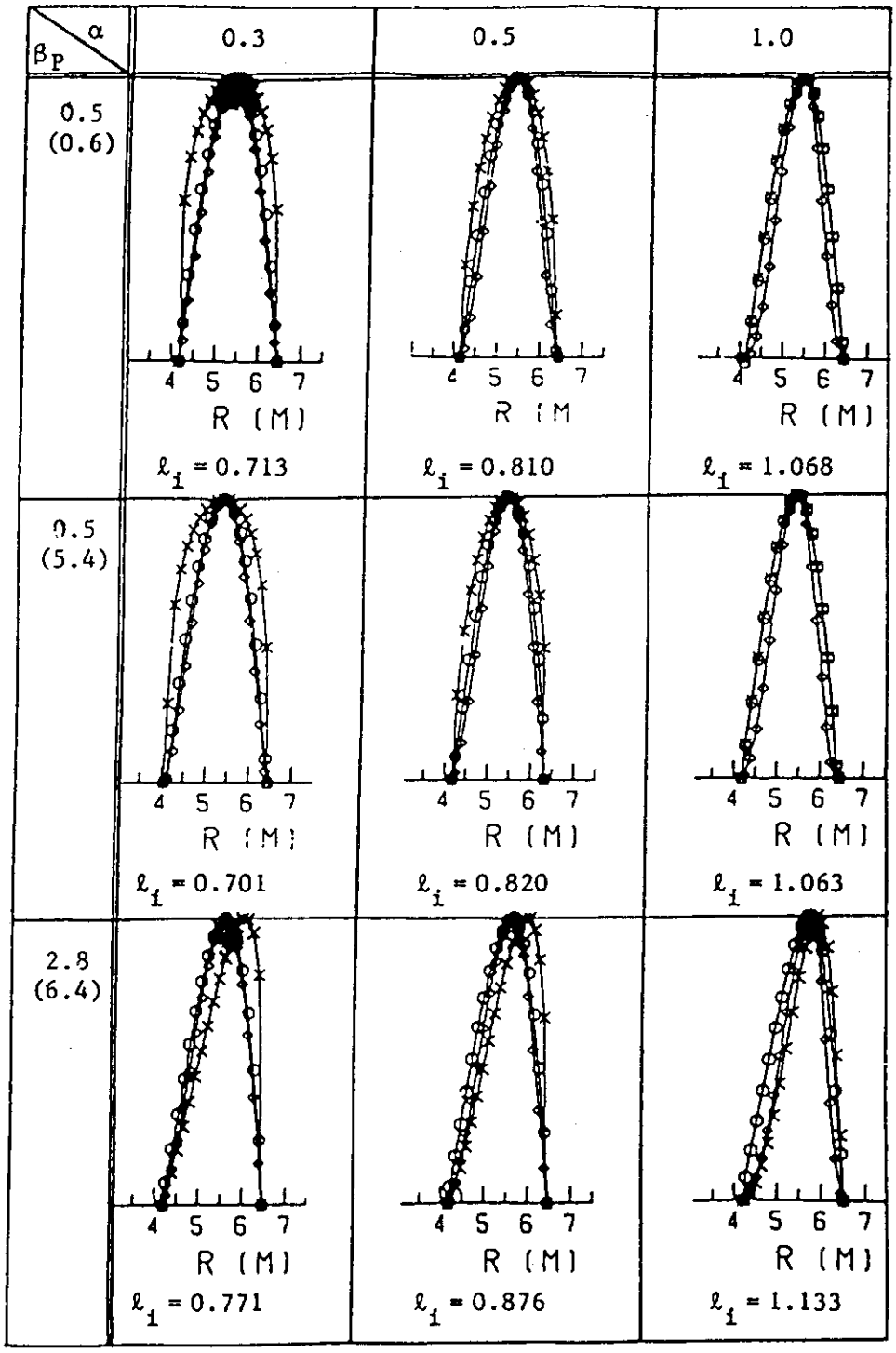

× Current Density, ◇ Plasma pressure,

○ Magnetic flux density

( ) : I_p(MA)

Table 2 INTOR equilibrium and EF field parameters with the PFCC in Fig.3(b)

Coil Number	Coordinates of Coil (m)		Ampere-turns (MAT)	
	Radial	Axial	$\beta_p = 0.1$	$\beta_p = 2.8$
1	1.40	-3.00	10.84	0.36
2	2.75	-6.90	3.14	7.06
3	4.00	-7.30	9.44	21.23
4	5.75	-7.40	2.82	6.34
5	12.00	-5.10	- 9.22	-18.77
6	1.40	-0.50	-11.75	- 8.77
7	1.40	0.50	-11.75	- 8.77
8	1.40	3.00	9.17	2.45
9	4.00	7.30	0.0	- 2.77
10	12.00	5.10	- 1.70	2.63
Total Ampere-turns (MAT)			69.8	79.2
Plasma Current (MA)			4.0	6.4
External Magnetic Flux, ψ_p (VS)			-26.2	-49.0
Coordinates of Null Point	Radial, R_N (m)		4.66	4.57
	Axial, Z_N (m)		- 1.92	- 1.81
Ellipticity	Upper, E_1		1.40	1.40
	Lower, E_2		1.50	1.60
Triangularity	Upper, γ_1		0.30	0.30
	Lower, γ_2		0.20	0.20

Table 3 Major parameters for the divertor with the PFCC in Fig.9 (The INTOR-J "Universal")

Parameters \ t(sec.)		0.0	5.0	11.0	211.0
Parameters \ β_p		0.0	0.5	2.8	2.8
Plasma Currents (MA)		0.0	5.40	6.40	6.4
Elongation	Upper	-	1.50	1.60	1.60
	Lower	-	1.60	1.60	1.60
Triangularity	Upper	-	-	0.20	0.20
	Lower	-	-	0.40	0.40
E Vertical Field (T)		-	-0.285	-0.500	-0.500
Decay Index		-	-2.03	-1.10	-1.10
Self Inductance (μH)		-	11.98	12.25	12.25
Normalized ℓ_i		-	0.93	0.80	0.80
EF Supplied Flux (VS)		-	-20.0	-50.0	-50.0
OH Supplied Flux (VS)		40.0	-15.3	0.0	-10.0
Inductive Flux (VS)		-	64.7	78.4	78.4
Resistive Flux (VS)		-	10.6	12.6	22.6
Total Flux Supply (VS)		40.0	-35.3	-50.0	-60.0
Total Ampere-Turns (MAT)		68.4	95.2	81.9	94.7
Stored Energy (GJ)		-	(16.7)*	(17.5)*	(17.5)*
Null Point (m)	R_N	-	4.78	4.65	4.65
	Z_N	-	1.69	1.71	1.71

* On EF only

Table 4 Ampere-turns with each poloidal coil corresponding to Table 3

(Divertor configuration with the INTOR-J "Universal")

(MAT)

Coil	Coordinates (m)		t = 0.0sec.	0.3sec.	11.0sec.	211.0sec.
NO.	Radial	Axial	I_p/β_p=0MA/0	5.4MA/0.5	6.4MA/2.8	6.4MA/2.8
1	1.35	0.35	3.673	-2.894	-2.886	-3.804
2	1.35	0.95	3.101	-2.675	-2.886	-3.661
3	1.35	1.55	3.391	-2.786	-2.886	-3.734
4	1.35	2.15	3.200	-2.713	-2.886	-3.686
5	1.35	2.75	3.381	-1.293	0.0	-0.845
6	1.35	3.35	3.113	-1.191	0.0	-0.778
7	1.35	3.95	3.701	-1.416	0.0	-0.925
8	1.35	4.55	3.937	-4.506	3.000	2.016
9	1.90	5.30	3.588	-1.372	0.0	-0.897
10	3.00	6.50	1.933	-0.740	0.0	-0.483
11	4.50	6.50	0.597	4.563	1.061	1.452
12	7.50	6.00	0.351	-0.134	0.0	-0.088
13	11.00	4.50	0.239	-0.276	-3.000	-3.060
14	1.35	-0.35	3.675	-2.895	-2.886	-3.805
15	1.35	-0.95	3.100	-2.675	-2.886	-3.661
16	1.35	-1.55	3.391	-2.786	-2.886	-3.734
17	1.35	-2.15	3.208	-2.716	-2.886	-3.688
18	1.35	-2.75	3.353	-2.772	-2.886	-3.724
19	1.35	-3.35	3.165	-1.211	0.0	-0.791
20	1.35	-3.95	3.605	-1.379	0.0	-0.901
21	1.35	-4.55	4.024	-1.539	0.0	-1.006
22	1.90	-5.30	3.617	-1.394	0.0	-0.904
23	3.00	-6.50	1.827	17.031	16.340	15.883
24	4.50	-6.50	0.645	17.483	16.340	16.179
25	7.50	-6.00	0.320	-0.122	0.0	-0.080
26	11.00	-4.65	0.267	-14.599	-15.670	-15.737
Total Ampere-turns(MAT)			68.40	95.15	81.93	94.68
Total Flux Supply (VS)			40.0	-35.3	-50.0	-60.0

Table 5 Ampere-turns of each PF coil, total sum of absolute currents and ψ_p with the INTOR "Universal" obtained from both of the "EF + OH" and "EF only" method

	Coordinates (m)		t = 0 sec.	t = 5 sec, I_p/β_p = 5.4MA/0.5		t=11.0 sec, I_p/β_p=6.4MA/0.5		t=211.0 sec, I_p/β_p=6.4MA/2.8	
	Radial	Axial	I_p/β_p=ONA/0.0	EF + OH	EF only	EF + OH	EF only	EF only (A)	EF only (B)
1	1.35	0.35	4.006	− 2.420	− 2.396	− 2.972	− 2.892	− 4.042	− 3.231
2	1.35	0.95	3.413	− 2.364	− 2.396	− 3.047	− 2.892	− 4.042	− 3.231
3	1.35	1.55	3.666	− 2.388	− 2.396	− 3.015	− 2.892	− 4.042	− 3.231
4	1.35	2.15	3.582	− 2.380	− 2.396	− 3.038	− 2.892	− 4.042	− 3.231
5	1.35	2.75	3.544	− 0.339	0.0	0.449	0.0	0.0	0.0
6	1.35	3.35	3.639	− 4.348	0.0	0.461	0.0	0.0	0.0
7	1.35	3.95	4.486	− 0.429	− 5.000	0.568	13.389	9.367	− 4.621
8	1.60	5.10	8.537	− 0.817	0.0	1.081	0.0	0.0	0.0
9	3.50	6.05	1.361	3.824	3.807	5.466	− 0.500	0.0	0.0
10	4.95	6.05	0.491	− 0.047	0.0	1.062	− 0.500	0.0	0.0
11	10.00	5.40	0.546	1.327	1.306	− 2.931	1.000	− 0.500	1.000
12	1.35	− 0.35	4.029	− 2.422	− 2.396	− 2.969	− 2.892	− 4.042	− 3.231
13	1.35	− 0.95	3.375	− 2.360	− 2.396	− 3.052	− 2.892	− 4.042	− 3.231
14	1.35	− 1.55	3.736	− 2.394	− 2.396	− 3.176	− 2.892	− 4.042	− 3.231
15	1.35	− 2.15	3.458	− 2.368	− 2.396	− 3.041	− 2.892	− 4.042	− 3.231
16	1.35	− 2.75	3.781	− 2.399	− 2.396	− 3.000	− 2.892	4.042	− 3.231
17	1.35	− 3.35	3.157	− 0.302	0.0	0.400	0.0	0.0	0.0
18	1.35	− 3.95	5.234	− 0.501	0.0	0.663	0.0	0.0	0.0
19	1.60	− 5.10	7.506	− 0.718	0.0	0.951	0.0	0.0	0.0
20	3.15	− 6.20	2.118	13.115	18.343	14.341	0.0	0.0	1.0
21	5.65	− 6.20	0.580	13.263	10.000	14.146	23.419	21.662	22.411
22	12.35	− 4.90	0.543	−17.689	−16.888	−19.558	−24.385	−22.853	−24.953
Total Ampere-turns (MAT)			74.79	78.22	76.91	89.39	89.22	90.76	83.06
Total Flux Supply (vs)			43.80	−28.07	−28.00	−46.20	−46.20	−56.20	−56.20

Table 6 Major Parameters for the divertor with the PFCC in Fig. 9 (The INTOR "Universal")

Parameters \ t(sec.)		0.0	5.0	11.0	211.0
Parameters \ β_p		0.0	0.5	2.8	2.8
Plasma Current (MA)		0.0	5.4	6.4	6.4
Elongation	Upper	–	1.6	1.6	1.6
	Lower	–	1.6	1.6	1.6
Triangularity	Upper	–	0.3	0.3	0.3
	Lower	–	0.2	0.2	0.2
E Vertical Field (T)		–	− 0.275	− 0.486	− 0.508
Decay Index		–	− 2.153	− 1.516	− 1.333
Self Inductance (μH)		–	11.33	12.08	12.36
Normalized ℓ_i		–	0.783	0.778	0.791
EF Supplied Flux (VS)		0.0	−25.20	−50.00	−56.2
OH Supplied Flux (VS)		43.8	− 2.87	3.80	0.0
Inductive Flux (VS)		0.0	61.18	77.31	79.10
Resistive Flux (VS)		0.0	10.69	12.69	20.90
Total Flux Supply (VS)		43.8	−28.07	−46.20	−56.20
Total Ampere-turns (MAT)		74.79	78.22	89.39	83.06
Null Point (m)	R_N	–	4.88	4.84	4.76
	Z_N	–	1.70	1.69	1.66

Table 7 Major parameters for the optimized PFCC for pump limiter in Fig.10

Parameters \ t(sec.)		0.0	0.30	5.0	11.0	211.0
β_p		0.0	0.50	0.50	2.80	2.80
Plasma Current (MA)		0.0	0.60	1.50	1.50	1.50
Elongation	Upper	-	0.60	5.40	6.40	6.40
	Lower	-	1.50	1.50	1.50	1.50
Triangularity	Upper	-	0.10	0.10	0.10	0.10
	Lower	-	0.15	0.15	0.15	0.15
E Vertical Field (T)		-	-0.030	-0.268	-0.511	-0.511
Decay Index		-	-1.566	-1.538	-0.999	-0.999
Self Inductance (μH)		-	11.32	11.30	12.68	12.68
Normalized ℓ_i		-	0.676	0.674	0.763	0.763
EF Supplied Flux (vs)		0.0	3.30	-26.17	-60.0	-60.0
OH Supplied Flux (vs)		40.0	26.70	-11.70	0.0	-10.0
Inductive Flux (vs)		0.0	6.79	61.02	81.15	81.15
Resistive Flux (vs)		0.0	3.21	16.85	18.85	28.85
Total Flux Supply (vs)		40.0	30.00	-37.87	-60.00	-70.00
Total Ampere-turns (MAT)		66.92	54.18	64.76	71.30	86.33

Table 8 Ampere-turns with each poloidal coil with the optimized PFCC for pump limiter in Fig.10

Coil No.	Coordinates(m)		t = 0 sec.	0.3 sec.	5.0 sec.	11.0 sec.	211. sec.
	Radial	Axial	I_p/β_p=0 MA/0	0.6 MA/0.5	5.4 MA/0.5	6.4 MA/2.8	0.4 MA/2.8
1	1.35	0.35	3.683	2.872	-2.564	-2.979	-3.900
2	1.35	0.95	3.108	2.489	-2.396	-2.979	-3.756
3	1.35	1.55	3.396	2.681	-2.480	-2.979	-3.828
4	1.35	2.15	3.217	2.562	-2.428	-2.979	-3.783
5	1.35	2.75	3.369	2.663	-2.473	-2.979	-3.821
6	1.35	3.35	3.180	2.537	-2.417	-2.979	-3.774
7	1.35	3.95	3.964	2.646	-1.159	0.0	-0.991
8	1.50	4.70	4.341	2.898	-1.270	0.0	-1.085
9	2.10	5.50	2.857	1.907	-0.836	0.0	-0.714
10	3.70	6.50	1.771	3.000	6.598	6.341	5.898
11	7.50	6.00	0.416	0.278	-0.122	0.0	-0.104
12	13.00	4.60	0.181	-0.452	-4.631	-7.302	-7.347
13	1.35	-0.35	3.677	2.869	-2.563	-2.979	-3.898
14	1.35	-0.95	3.117	2.495	-2.399	-2.979	-3.758
15	1.35	-1.55	3.377	2.668	-2.475	-2.979	-3.823
16	1.35	-2.15	3.248	2.582	-2.437	-2.979	-3.791
17	1.35	-2.75	3.312	2.625	02.456	-2.979	-3.807
18	1.35	-3.35	3.280	2.603	2.446	-2.979	-3.799
19	1.35	-3.95	3.779	2.522	-1.105	0.0	-0.945
20	1.50	-4.70	4.568	3.049	-1.336	0.0	-1.142
21	2.10	-5.50	2.787	1.860	-0.815	0.0	-0.697
22	3.70	-6.50	1.624	3.340	11.997	13.179	12.773
23	7.50	-6.00	0.421	0.281	-0.123	0.0	-0.105
24	13.00	-3.60	0.249	-0.299	-5.234	-8.732	-9.794
Total Ampere-turns(MAT)			66.92	54.18	64.76	71.30	86.33
Total Flux Supply(VS)			40.00	30.00	-37.87	-60.00	-70.00

* $R_{12} = R_{24} = 13$ m (Pump Limiter Type)

Table 9 Major parameters for the pump limiter with the PFCC in Fig. 15 (THE INTOR "Universal")

Parameters \ t(sec.) / β_p		0.0	0.30	5.0	11.0	221.0
		0.0	0.50	0.50	2.80	2.80
Plasma Current (MA)		0.0	0.60	5.40	6.40	6.40
Elongation	Upper	–	1.50	1.50	1.50	1.50
	Lower	–	1.50	1.50	1.50	1.50
Triangularity	Upper	–	0.15	0.15	0.15	0.15
	Lower	–	0.15	0.15	0.15	0.15
E Vertical Field (T)		–	−0.0298	− 0.266	− 0.513	− 0.513
Decay Index		–	−1.431	− 1.465	− 1.015	− 1.015
Self Inductance (μH)		–	11.16	11.18	12.70	12.70
Normalized ℓ_i		–	0.683	0.669	0.757	0.757
EF Supplied Flux (VS)		0.0	4.03	−22.32	−55.92	−55.92
OH Supplied Flux (VS)		43.8	27.85	−12.89	− 2.20	−12.20
Inductive Flux (VS)		0.0	6.70	60.37	81.28	81.28
Resistive Flux (VS)		0.0	3.30	16.72	18.72	28.72
Total Flux Supply (VS)		43.8	31.88	−35.21	−58.12	−68.12
Total Ampere-turns (MAT)		74.79	56.65	63.06	77.06	92.05

★ Limiter Point (4.90^m, -1.30^m)

Table 10 Ampere-turns with each poloidal coil corresponding to Table 9 (Pump limiter configuration with the INTOR "Universal")

(MAT)

NO.	Coordinates (m)		t = 0 sec.	0.3 sec.	5.0 sec.	11.0 sec.	211.0 sec.
	Radial	Axial	I_p/β_p=0MA/0.0	0.6MA/0.5	5.4MA/0.5	6.4MA/2.8	6.4MA/2.8
1	1.35	0.35	4.006	3.034	− 2.337	− 2.996	− 3.910
2	1.35	0.95	3.413	2.658	− 2.162	− 2.966	− 3.745
3	1.35	1.55	3.666	2.818	− 3.165	− 2.979	− 3.816
4	1.35	2.15	3.582	2.765	− 2.212	− 2.975	− 3.793
5	1.35	2.75	3.544	2.741	− 2.201	− 2.973	− 3.782
6	1.35	3.35	3.639	2.801	− 2.229	− 2.978	− 3.808
7	1.35	3.95	4.486	2.852	− 1.320	− 0.225	− 1.249
8	1.60	5.10	8.537	5.427	− 2.512	− 0.429	− 2.377
9	3.50	6.05	1.361	1.644	3.613	4.929	4.618
10	4.95	6.05	0.491	1.091	3.869	4.972	4.860
11	10.00	5.40	0.546	0.001	− 3.997	− 7.168	− 7.293
12	1.35	−0.35	4.029	3.049	− 2.343	− 2.997	− 3.917
13	1.35	−0.95	3.375	2.633	− 2.151	− 2.964	− 3.735
14	1.35	−1.55	3.736	2.863	− 2.257	− 2.983	− 3.835
15	1.35	−2.15	3.458	2.686	− 2.175	− 2.969	− 3.758
16	1.35	−2.75	3.781	2.891	− 2.270	− 2.985	− 3.848
17	1.35	−3.35	3.157	2.495	− 2.087	− 2.954	− 3.674
18	1.35	−3.95	5.234	3.327	− 1.540	− 0.263	− 1.457
19	1.60	−5.10	7.506	4.772	− 2.208	− 0.377	− 2.090
20	3.15	−6.20	2.118	2.262	4.040	5.335	4.851
21	5.65	−6.20	0.580	1.285	4.492	5.412	5.280
22	12.35	−4.9	0.543	− 0.554	− 7.785	−12.228	−12.352
Total Ampere-turns (MAT)			74.79	56.65	63.06	77.06	92.05
Total Flux Supply (VS)			43.81	27.85	−35.21	−58.12	−68.12

Table 11 Major Parameters for the pump limiter with the PFCC in Fig. 9 (The INTOR-J "Universal")

Parameters \ t(sec.) / β_p		0.0	0.3	5.0	11.0	211.0
		0.0	0.5	0.5	2.8	2.8
Plasma Current (MA)		0.0	0.6	5.4	6.4	6.4
Elongation	Upper	–	1.5	1.5	1.5	1.5
	Lower	–	1.5	1.5	1.5	1.5
Triangularity	Upper	–	0.15	0.15	0.15	0.15
	Lower	–	0.15	0.15	0.15	0.15
E Vertical Field (T)		–	−0.0303	− 0.267	− 0.513	− 0.513
Decay Index		–	−1.582	− 1.471	− 1.019	− 1.021
Self-Inductance (μH)		–	11.55	11.19	12.71	12.71
Normalized ℓ_i		–	0.765	0.670	0.757	0.755
EF Supplied Flux (VS)		0.0	3.23	−26.07	−60.0	−70.0
OH Supplied Flux (VS)		40.0	26.77	−11.02	0.0	0.0
Inductive Flux (VS)		0.0	6.93	60.43	81.34	81.34
Resistive Flux (VS)		0.0	3.07	16.66	18.66	28.66
Total Flux Supply (VS)		40.0	30.00	−37.09	−60.0	−70.0
Total Sum, $\Sigma\|NI\|$ (MAT)		68.4	55.42	65.55	80.02	87.95
Limiter Point (m)	R_L	–	4.90	4.90	4.90	4.90
	Z_L	–	1.30	1.30	1.30	1.30

Table 12 Ampere-turns with each poloidal coil corresponding to Table 11 (The INTOR-J "Universal")

NO.	Coordinates (m)		t = 0 sec.	0.3 sec.	5.0 sec.	11.0 sec.	211.0 sec.
	Radial	Axial	I_p/β_p=0MA/0	0.6MA/0.5	5.4MA/0.5	6.4MA/2.8	6.4MA/2.8
1	1.35	0.35	3.673	2.848	− 2.569	− 3.258	− 4.159
2	1.35	0.95	3.101	2.465	− 2.412	− 3.258	− 4.159
3	1.35	1.55	3.391	2.659	− 2.492	− 3.258	− 4.159
4	1.35	2.15	3.200	2.532	− 2.439	− 3.258	− 4.159
5	1.35	2.75	3.381	2.653	− 2.489	− 3.258	− 4.159
6	1.35	3.35	3.113	2.473	− 2.415	− 3.258	− 4.159
7	1.35	3.95	3.701	2.477	− 1.020	0.0	0.0
8	1.35	4.55	3.937	2.635	− 1.085	0.0	0.0
9	1.90	5.30	3.588	2.401	− 0.988	0.0	0.0
10	3.00	6.50	1.933	2.383	4.415	5.936	5.207
11	4.50	6.50	0.597	1.488	4.783	5.936	5.207
12	7.50	6.00	0.351	0.235	− 0.097	0.0	0.0
13	11.00	4.50	0.239	−0.373	− 4.750	− 8.363	− 8.395
14	1.35	−0.35	3.675	2.849	− 2.570	− 3.258	− 4.159
15	1.35	−0.95	3.100	2.465	− 2.412	− 3.258	− 4.159
16	1.35	−1.55	3.391	2.659	− 2.492	− 3.258	− 4.159
17	1.35	−2.15	3.208	2.537	− 2.441	− 3.258	− 4.159
18	1.35	−2.75	3.358	2.637	− 2.483	− 3.258	− 4.159
19	1.35	−3.35	3.165	2.508	− 2.429	− 3.258	− 4.159
20	1.35	−3.95	3.605	2.413	− 0.993	0.0	0.0
21	1.35	−4.55	4.024	2.693	− 1.109	0.0	0.0
22	1.90	−5.30	3.617	2.421	− 0.996	0.0	0.0
23	3.00	−6.50	1.827	2.373	4.914	6.070	5.330
24	4.50	−6.50	0.645	1.581	5.240	6.070	5.330
25	7.50	−6.00	0.320	0.214	− 0.088	0.0	0.0
26	11.00	−4.65	0.267	−0.445	− 5.430	− 8.557	− 8.570
$\Sigma \mid NI \mid$ (MAT)			68.40	55.42	65.55	80.02	87.95
ψ_p (vs)			40.0	30.0	−37.09	−60.0	−70.0

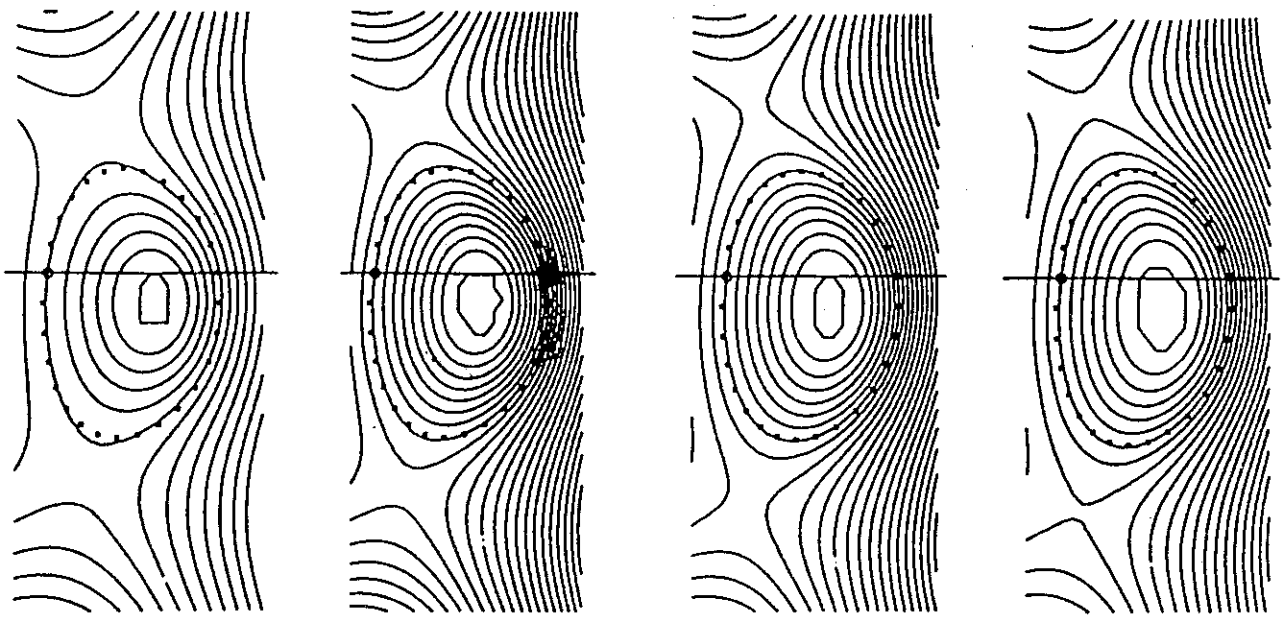

Fig. 1 Rélation of looped flux surfaces near the plasma with form factor, α on high beta

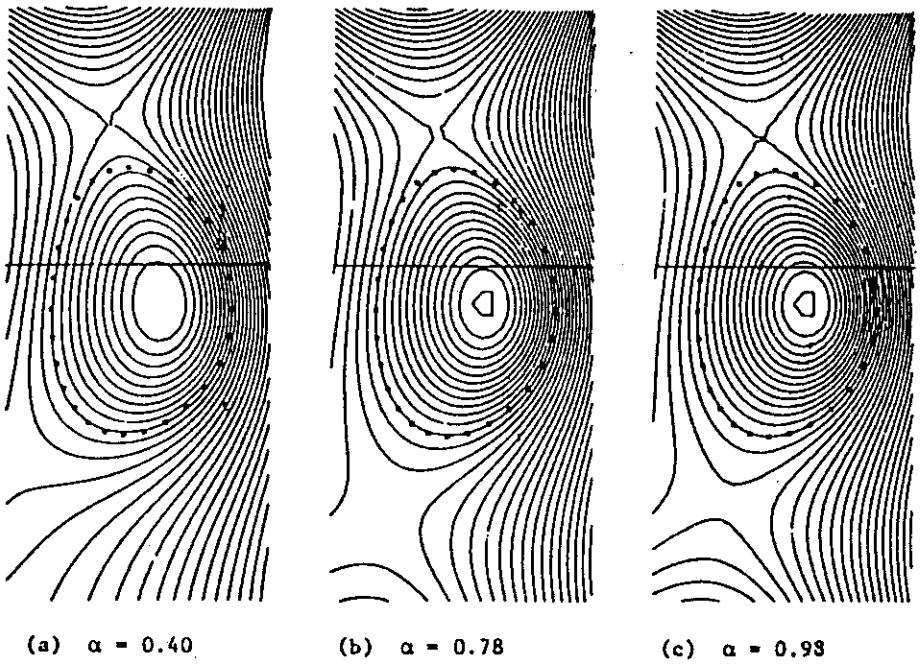

Fig. 2 Variation of separatrix and magnetic flux surfaces near the plasma for form factor, α on high beta

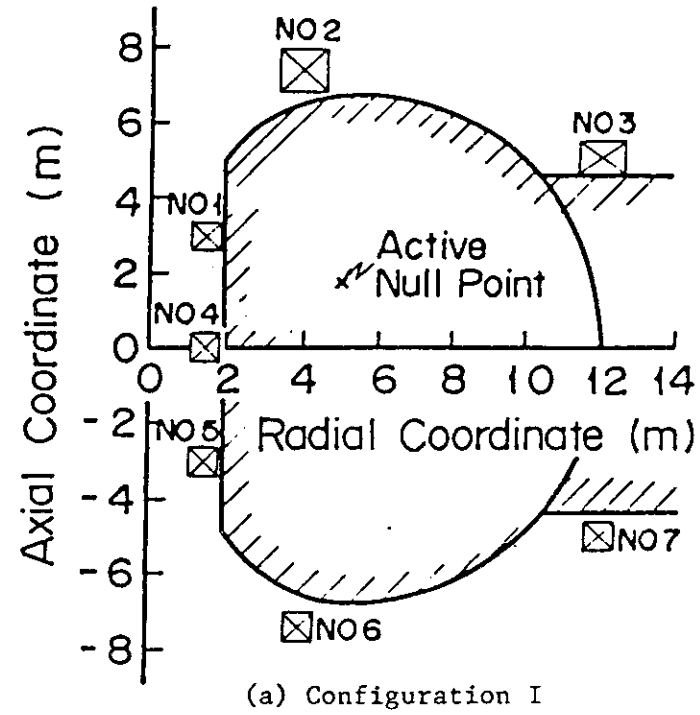

(a) Configuration I

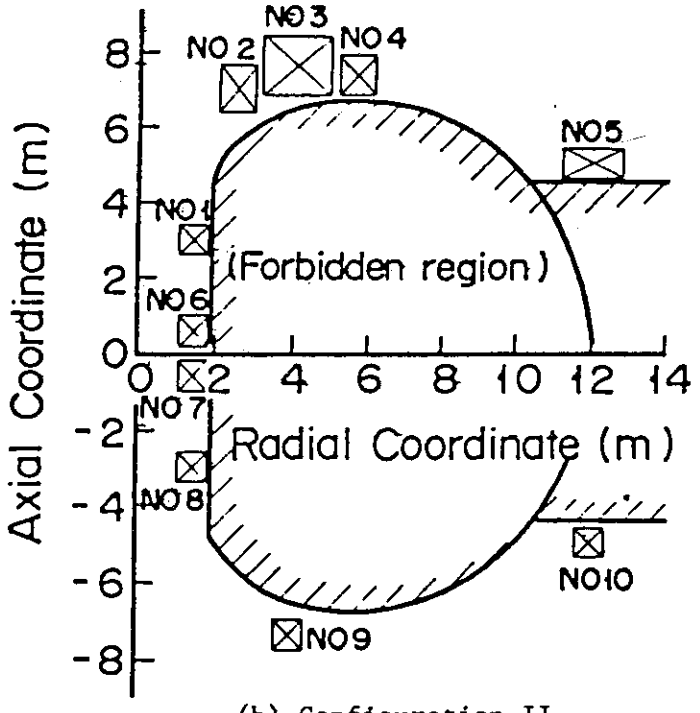

(b) Configuration II

Fig. 3 Simplified view of the PFCC on the beginning of the INTOR Phase I

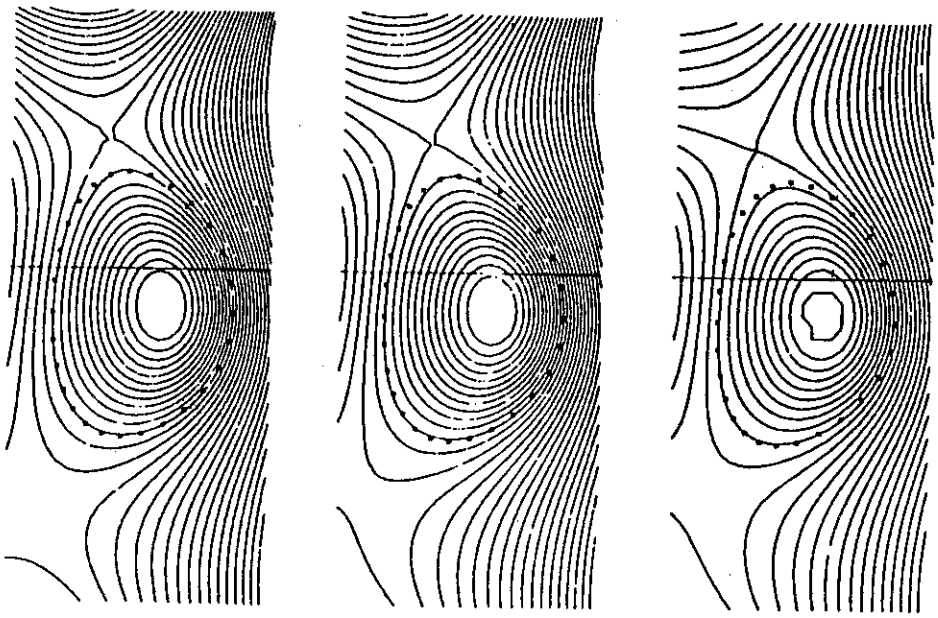

(a) $\gamma_1 = 0.225$, $\gamma_2 = 0.20$ (b) $\gamma_1 = 0.25$, $\gamma_2 = 0.20$ (c) $\gamma_1 = 0.30$, $\gamma_2 = 0.20$

Fig. 4 Variation of separatrix and magnetic flux surfaces near the plasma as a function of its lower trianguarrity, γ_1 with fixed parameters: $\gamma_2 = 0.20$, $K_1 = 1.40$ and $K_2 = 1.60$.

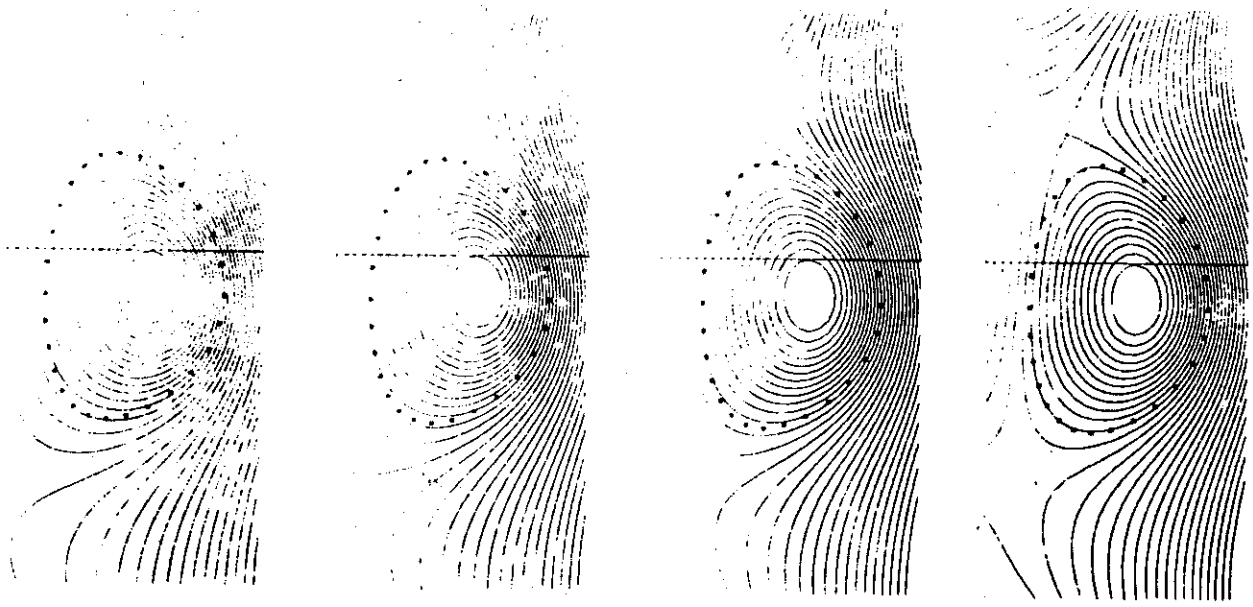

(a) $N_5I_5 = 3.0$, $N_6I_6 = -3.0$, $N_7I_7 = 3.0$ (b) 4.0, -4.0, 4.0 (c) 5.0, -5.0, 5.0 (d) 7.5 MAT, -6.0 MAT, 6.0 MAT

Fig. 5 Variation of separatrix and magnetic flux surfaces near the plasma as a function of ampere-turns of the Nos.5, 6 and 7 coils in Fig.3(a)

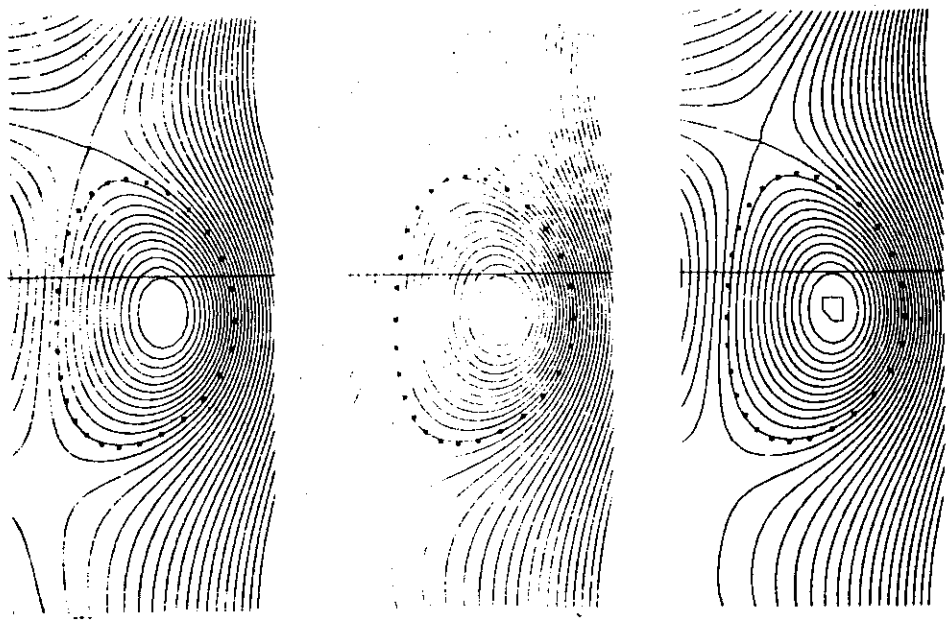

(a) $\Sigma\ (NI)^2 = 4 \times 10^{14}(AT)^2$ (b) $\Sigma\ (NI)^2 = 2 \times 10^{15}(AT)^2$ (c) $\Sigma\ (NI)^2 = 3 \times 10^{15}(AT)^2$

Fig. 6 Variation of separatrix and magnetic flux surfaces near the plasma as a function of the total sum, $\Sigma(NI)^2$, of the square ampere-turns with EF coils in Fig.3(a)

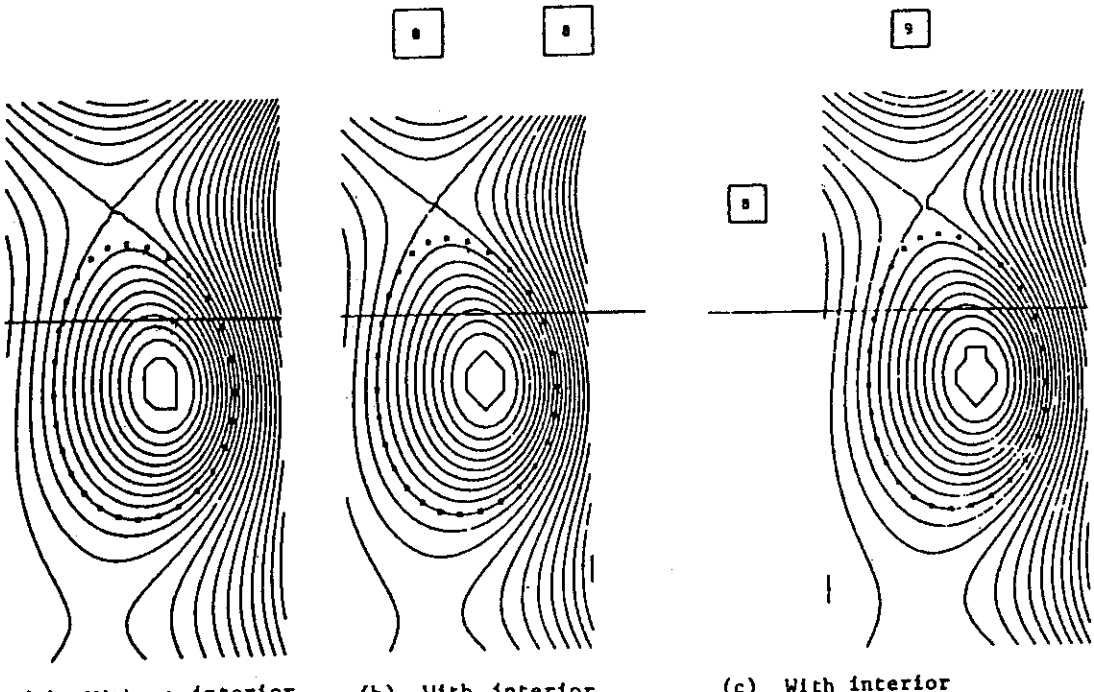

(a) Without interior coils (b) With interior coils-type A (c) With interior coils-type B

Fig. 7 Comparison of separatrix and magnetic flux surfaces near the plasma without and with a pair of coils of two kinds of types, A and B, inside the TF coil contour and near the plasma

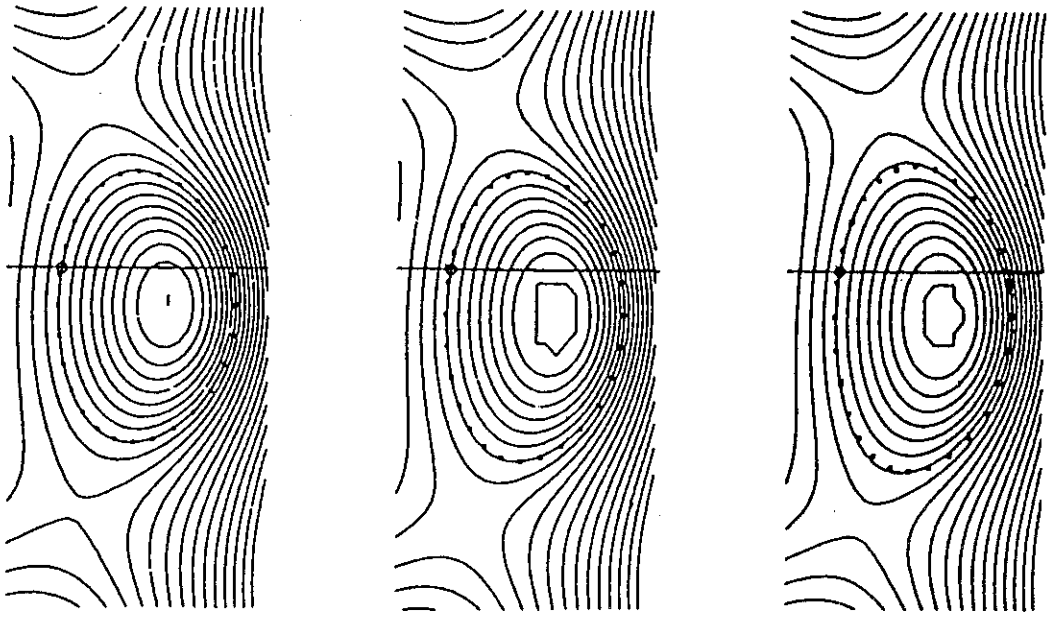

(a) K = 1.50 (b) K = 1.60 (c) K = 1.70

Fig. 8 Dependence of looped flux surfaces near the plasma of pump limiter upon its elongation

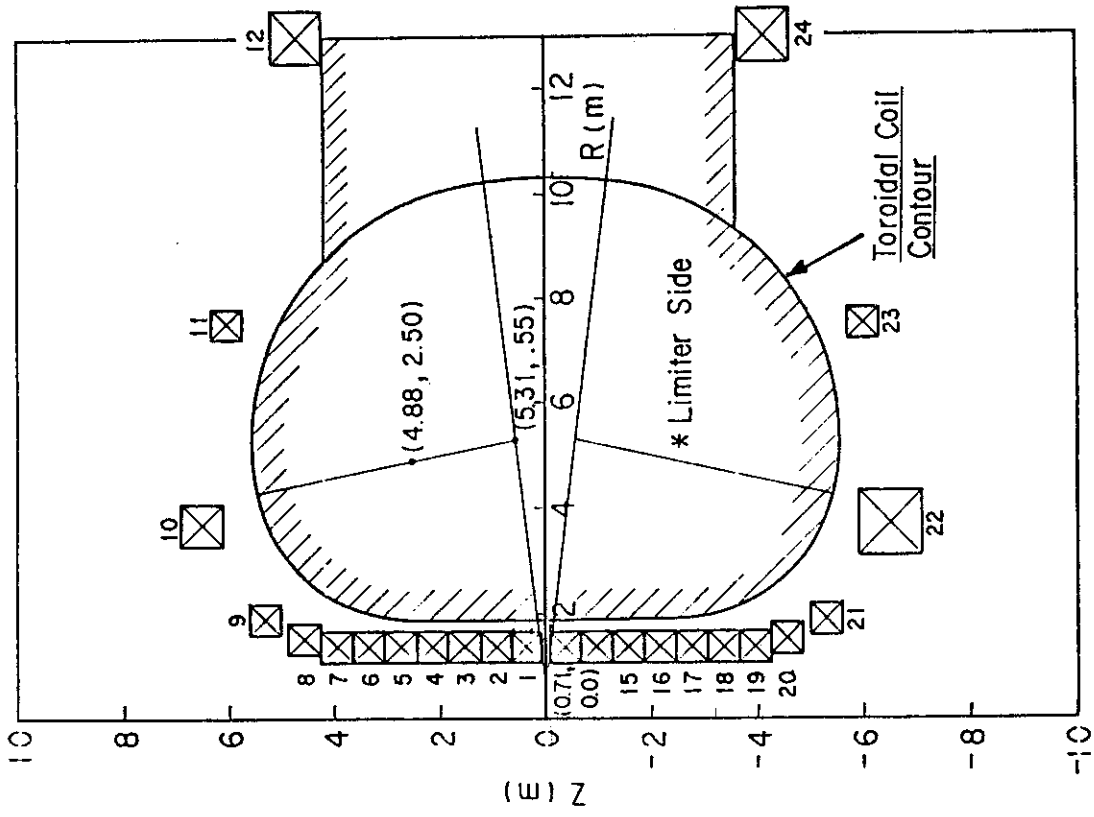

Fig.10 The PFCC optimized for the pump limiter configuration

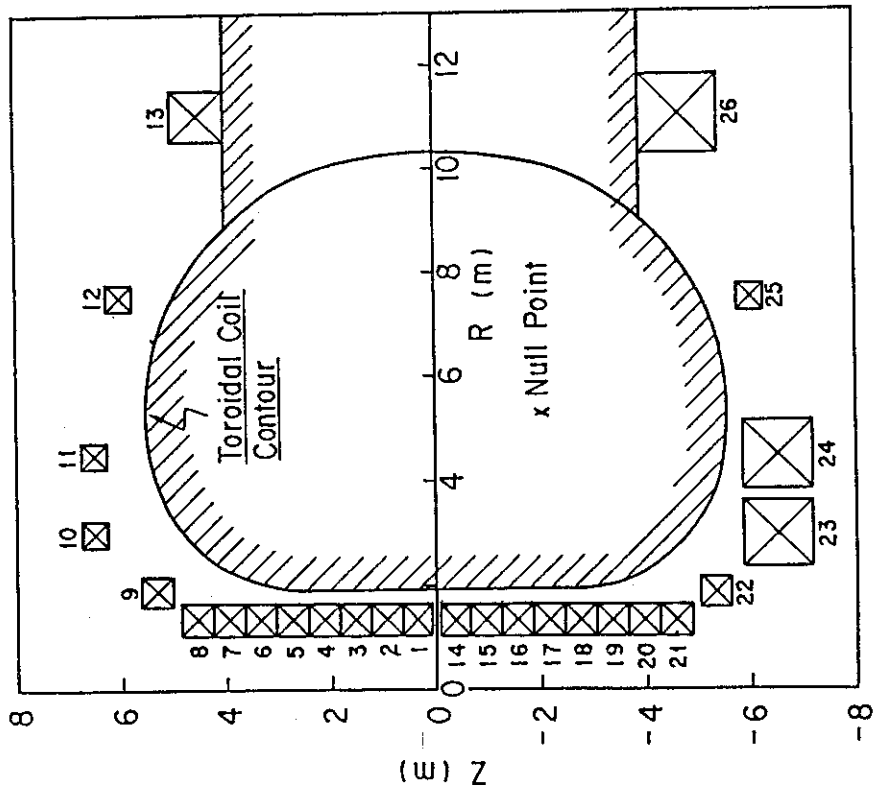

Fig. 9 The poloidal field coil configuration (PFCC) optimized for the divertor configuration (The INTOR-J "Universal")

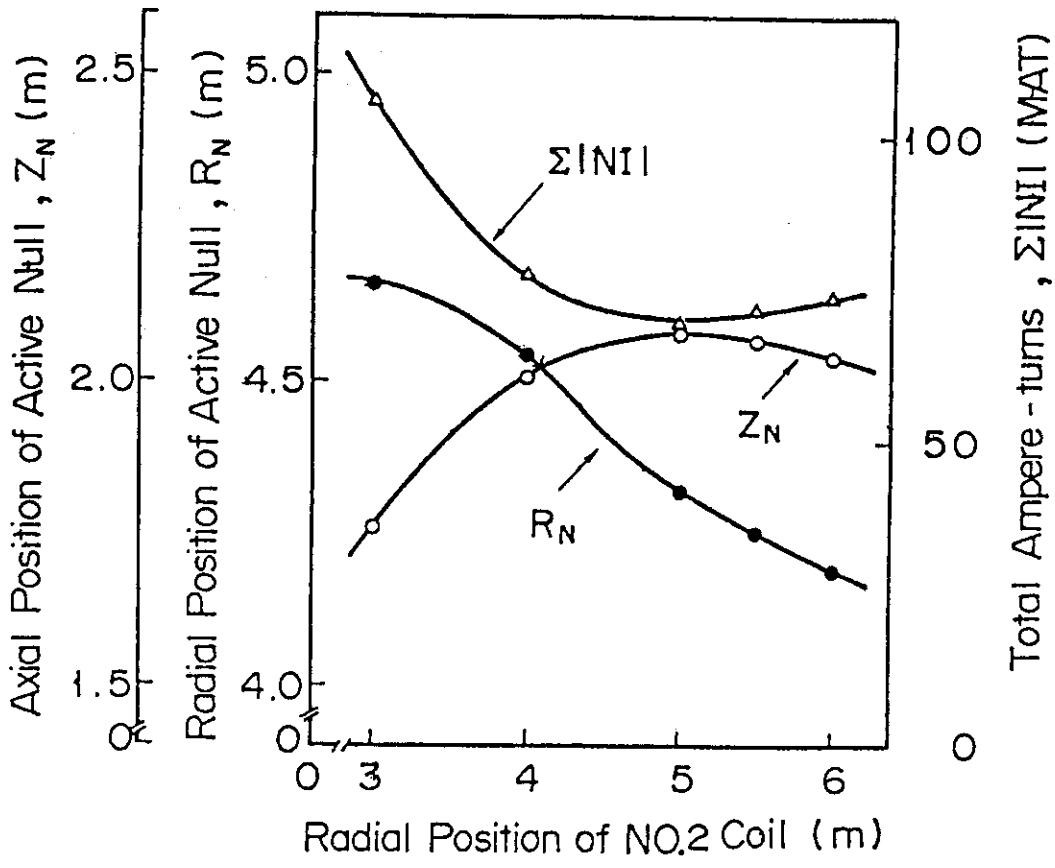

Fig.11 Dependence of active null position, (R_N,Z_N) and total sum of absolute currents, Σ|NI| on high beta upon the radial position of the No.2 coils with the PFCC in Fig.3(a)

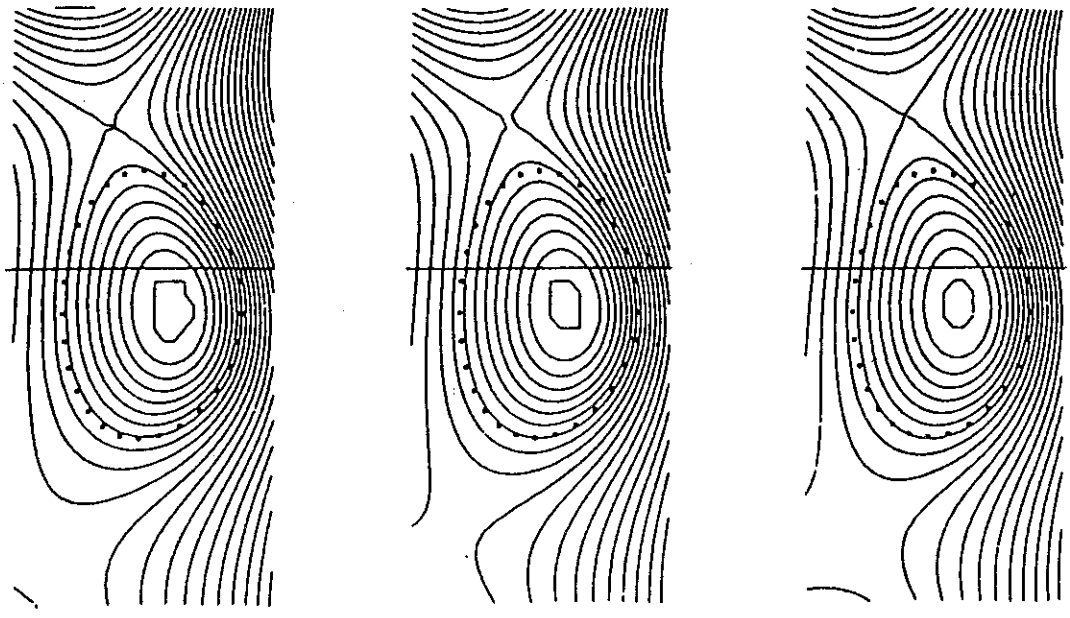

(a) $R_{13}=R_{26}=11m$ (b) $R_{13}=R_{26}=12m$ (c) $R_{13}=R_{26}=13m$

Fig.12 Dependence of magnetic flux surfaces and separatrix shape with the plasma upon the radial coordinate of large coils with fixed axial coordinate, on the PFCC in Fig.9

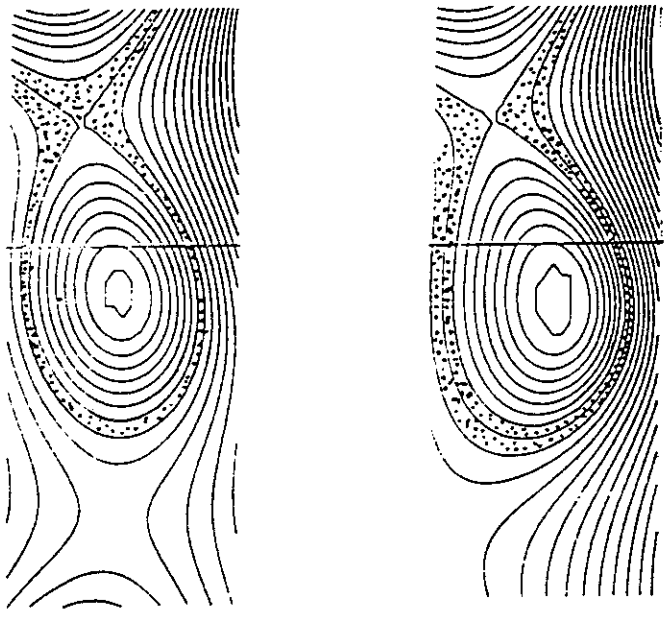

(a) I_P = 5.4 MA, β_P = 0.5 (b) I_P = 6.4 MA, β_P = 0.5

Fig.13 Plasma equilibrium on low and high beta for the divertor configuration with the PFCC in Fig.9 (The INTOR-J "Universal")

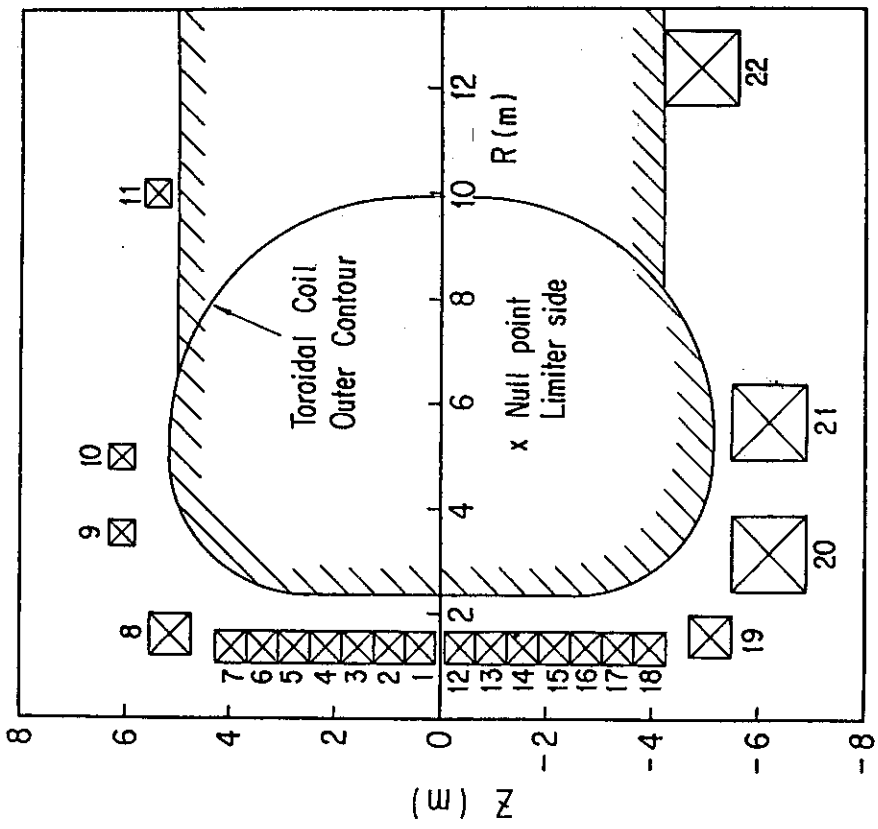

Fig.15

The PFCC presented on the final stage of the Phase II A (The INTOR "Universal")

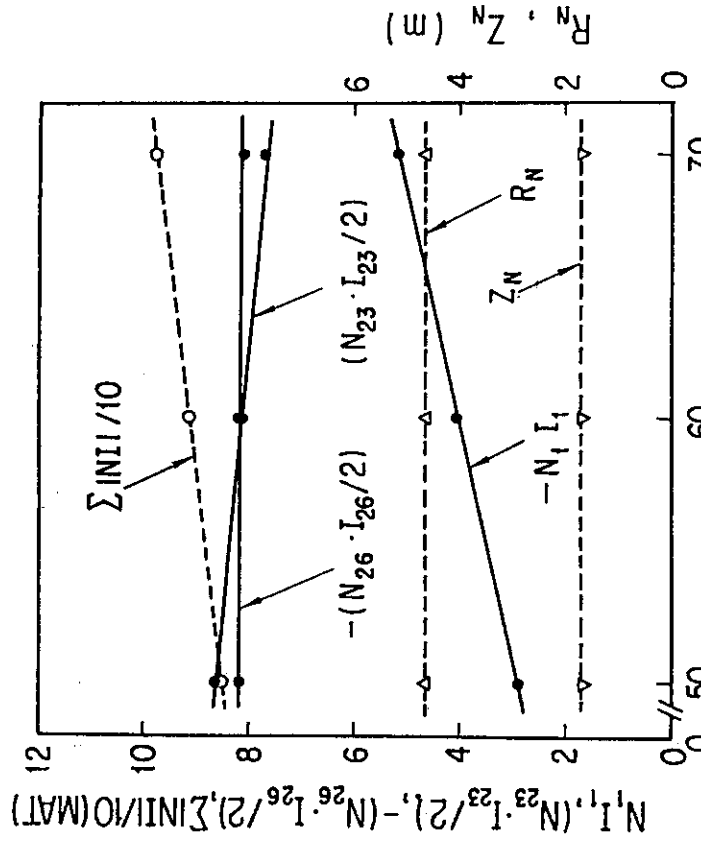

Fig.14

Variation of typical parameters, that is, (R_N,Z_N), N_1I_1, $N_{23}\cdot I_{23}$, $N_{26}\cdot I_{26}$ and $\Sigma|NI|$ with the high beta plasma as a function of ψ_p for the divertor configuration with the PFCC in Fig.9 (The INTOR-J "Universal")

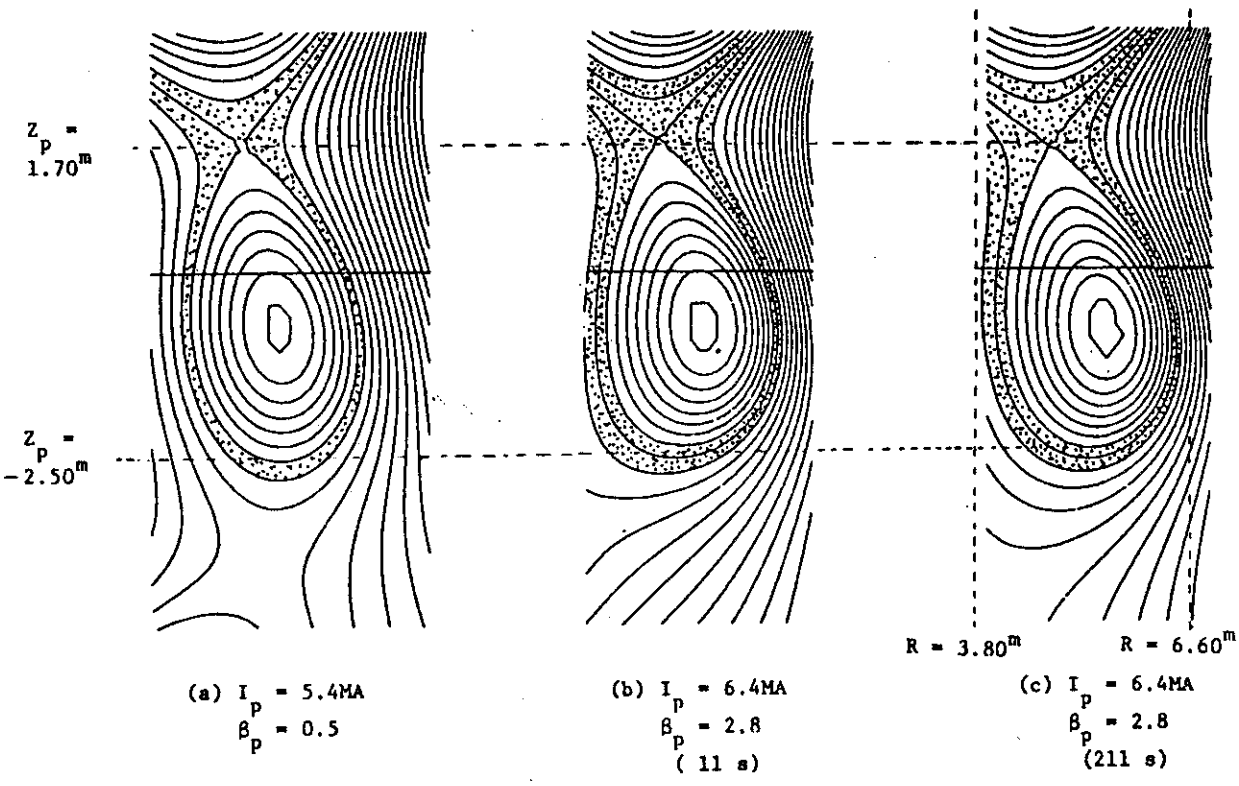

Fig.16 Plasma equilibrium on low and high beta for the divertor configuration with the PFCC in Fig.15 (The INTOR "Universal")

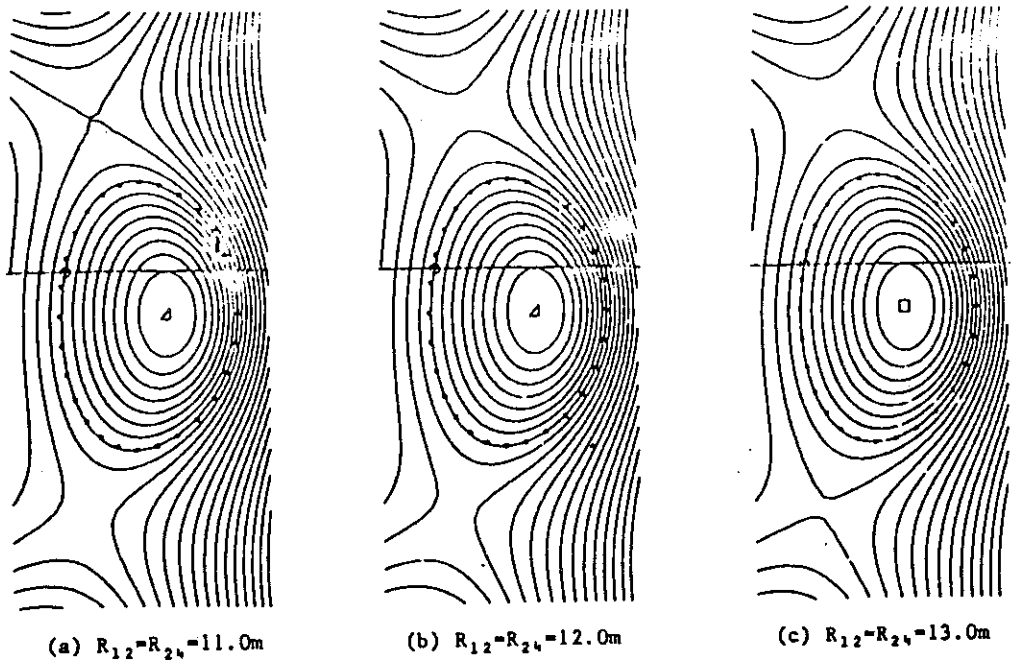

Fig.17 Dependence of looped flux surfaces near the high beta plasma upon the radial coordinate of large coils with its fixed axial coordinate with the PFCC in Fig.10

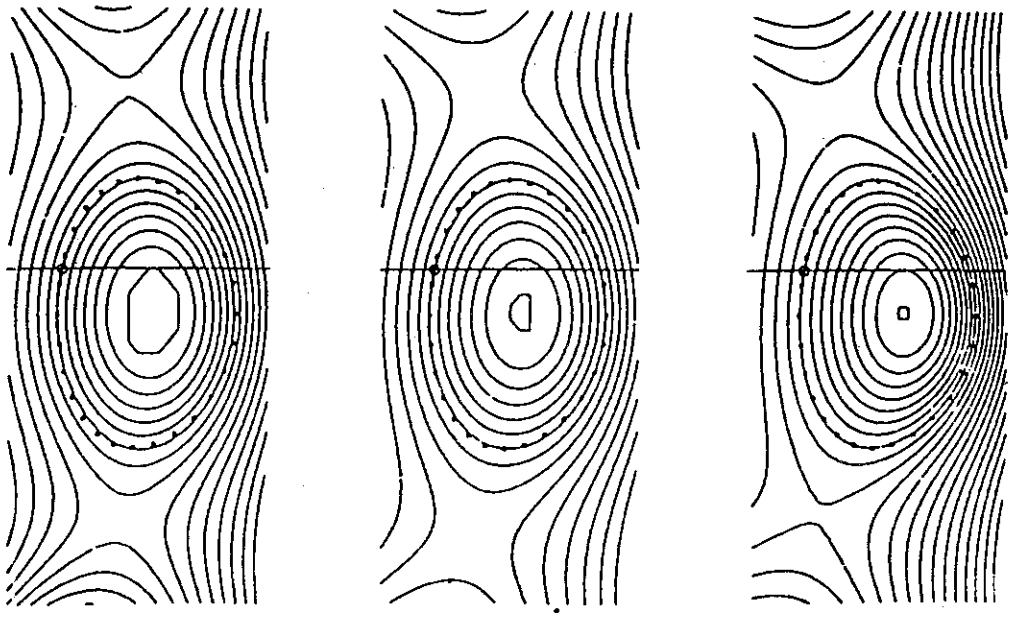

(a) I_p = 0.6MA, β_p = 0.5 (b) I_p = 5.4MA, β_p = 0.5 (c) I_p = 6.4MA, β_p = 2.8

Fig.18 Plasma equilibrium on low and high beta for the pump limiter configuration with the PFCC in Fig.10, and its reference of 1.5 in elongation

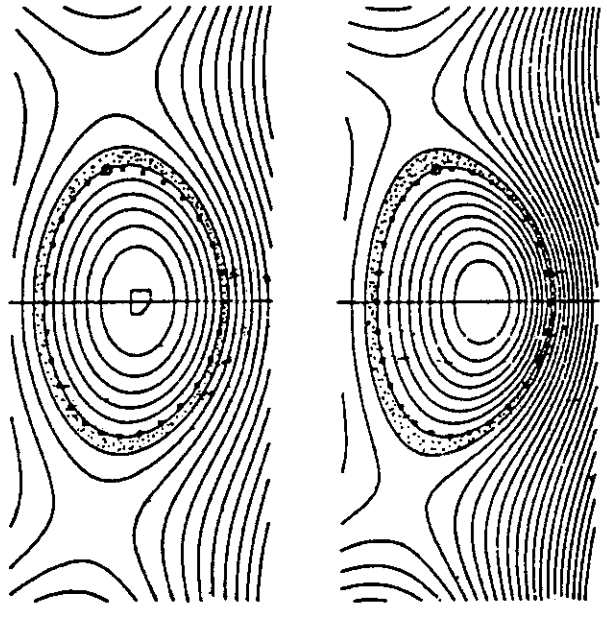

(a) I_p = 5.4MA, β_p = 0.5 (b) I_p = 6.4MA, β_p = 2.8

Fig.19 Plasma equilibrium on low and high beta for the pump limiter configuration with the PFCC in Fig.15, and its reference of 1.5 in elongation (The INTOR "Universal")

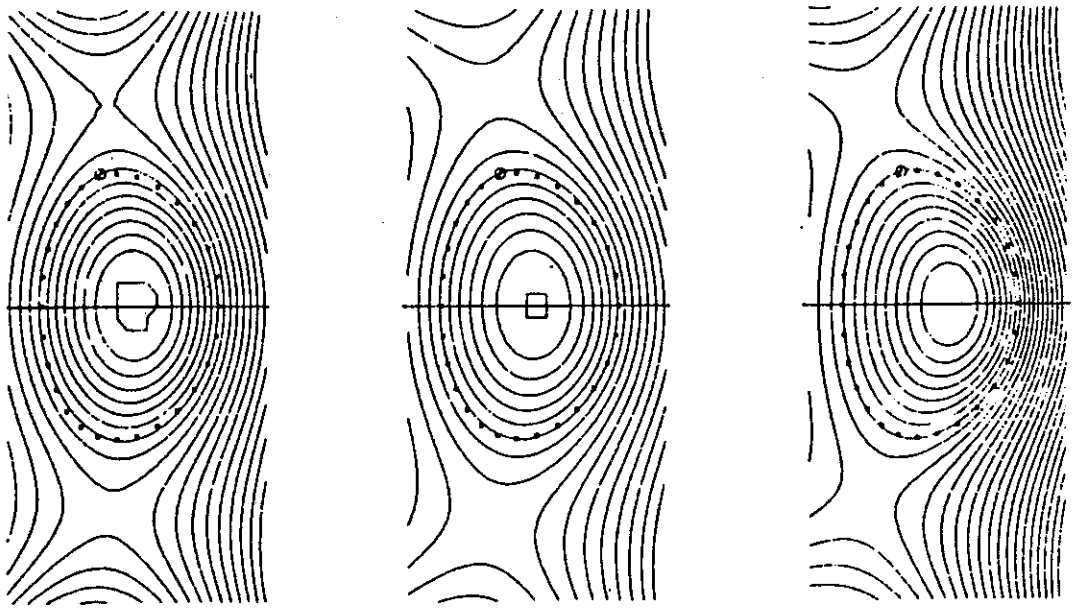

(a) I_p = 0.6MA, β_p = 0.5 (b) I_p = 5.4MA, β_p = 0.5 (c) I_p = 6.4MA, β_p = 2.8

Fig. 20 Plasma equilibrium on low and high beta for the pump limiter configuration with the PFCC in Fig.9 (The INTOR-J "Universal")

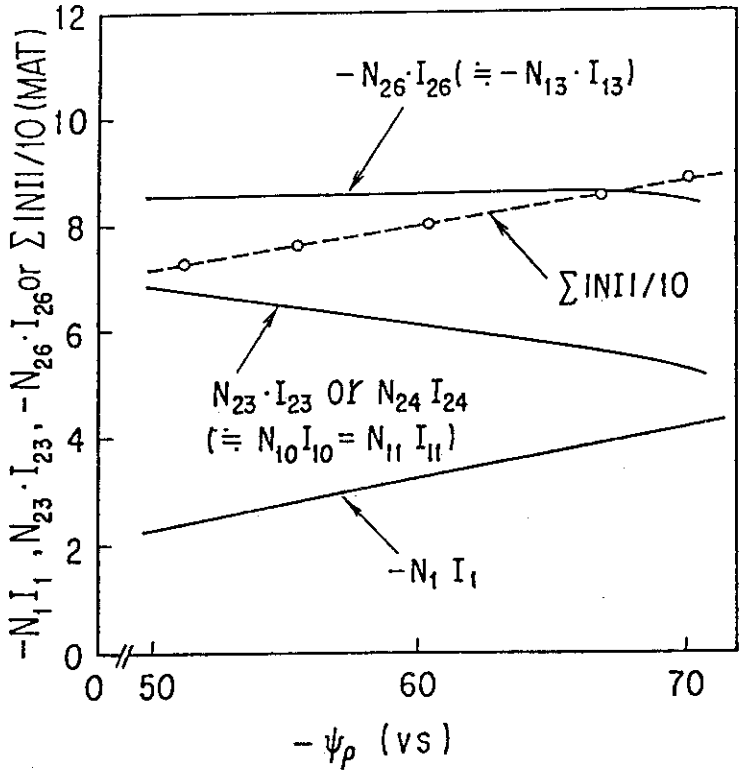

Fig. 21 Variation of typical parameters, that is, N_1I_1, $N_{23}\cdot I_{23}$, $N_{26}\cdot I_{26}$ and $\Sigma|NI|$ with high beta plasma as a function of Ψ_p for the pump limiter configuration with the PFCC in Fig.9 (The INTOR-J "Universal")